Theoretical Population Biology **54**, 270–293 (1998)
Article No. TP981380

TPB

Ontogenetic Scaling of Foraging Rates and the Dynamics of a Size-Structured Consumer-Resource Model

Lennart Persson and Kjell Leonardsson

Department of Animal Ecology, University of Umeå, Umeå S-90187, Sweden
E-mail: Lennart.Persson@animecol.umu.se

André M. de Roos

Department of Pure and Applied Ecology, University of Amsterdam, Kruislaan 320, Amsterdam NL-1098 SM, The Netherlands
E-mail: aroos@bio.uva.nl

Mats Gyllenberg

Department of Applied Mathematics, University of Turku, Turku FIN-20500, Finland
E-mail: matsgyl@utu.fi

and

Bent Christensen

Department of Animal Ecology, University of Umeå, Umeå S-90187, Sweden

Received July 4, 1997

The ontogenetic scaling of foraging capacity strongly influences the competitive ability of differently sized individuals within a species. We develop a physiologically structured model to investigate the effect of different ontogenetic size scalings of the attack rate on the population dynamics of a consumer-resource system. The resource is assumed to reproduce continuously whereas the consumer only reproduces at discrete time instants. Depending on the ontogenetic size scaling, the model exhibited recruit-driven cycles, stable fixed point dynamics, non-recruit juvenile-driven cycles, quasiperiodic orbits, or chaotic dynamics. The kind of dynamics observed was related to the maintenance resource levels required of differently sized individuals. Stable fixed point dynamics was, besides at the persistence boundary, only observed when the minimum resource levels were similar for newborns and mature individuals. The tendency for large population fluctuations over a wide range of the parameter space was due to the consumer's pulsed reproduction. Background mortality and length of season were major determinants of cycle length. Model dynamics strongly resembled empirically observed dynamics from fish and *Daphnia* populations with respect to both patterns and mechanisms. The non-recruit juvenile-driven dynamics is suggested to occur in populations with size-dependent interference or preemptive competition like cicada populations. © 1998 Academic Press

0040-5809/98 $25.00

1. INTRODUCTION

Organisms of most animal taxa undergo growth and morphological change during a substantial part of the life cycle. Due to the taxonomic dominance of insects and marine phyla, Werner (1988) estimated that approximately 80% of all animal species undergo metamorphosis. Even if only vertebrates are considered, individuals of 75% of all taxa grow during most of their life cycle (Ebenman and Persson, 1988). The rate at which the organism grows often depends on resource levels and observed variations in size structure between populations can in many cases be related to resource dependent individual growth (Norberg, 1988; Persson, 1988; Wilbur, 1988).

The phenomenon of individual growth entails that two fundamental components of its competitive ability, its foraging rate and its metabolic demands, change over the organism's life cycle where the competitive ability is defined by (1) the ability of the individual to consume the resource and (2) its ability to withstand resource depression (depending on metabolic demands). (Persson, 1985; Werner, 1988; Lundberg and Persson, 1993). Changes in these components are expected to have major impacts on ecological interactions as size-dependent foraging capacity has been shown to have major effects on habitat use and performance of differently sized individuals (Mittelbach, 1981; Werner *et al*., 1983; Persson, 1987). An analysis of how size-dependent changes in the two components of competitive ability over ontogeny affect population dynamics is therefore of major importance in order to increase our understanding of ecological interactions in natural systems.

Of the two components, metabolic demands have been found to scale to body weight according to a power function with an exponent generally varying between 0.7 and 0.8 between taxa (Peters, 1983; Calder, 1984). The foraging rate as a function of body weight is also commonly described by a power function (Schoener, 1969; Wilson, 1975; Peters, 1983; Calder, 1984; Werner, 1988). However, this intraspecific scaling of foraging rate to body size (hereafter the ontogenetic scaling of foraging rate) varies much more between different taxa than the corresponding exponent for metabolic demands (Werner 1988). Reasons for this are that the foraging rate of an organism is the integrated result of a number of traits (visual acuity, locomotor ability, gape size and digestive capacity) each of which exhibits substantially different ontogenetic scaling relations in different taxa (Schoener, 1969; Wilson, 1975; Peters, 1983; Calder, 1984; Hyatt, 1979; Sebens, 1982; Hoyle and Keast, 1987; Persson, 1987).

The effects of the ontogenetic scaling relation, and changes therein, on the competitive abilities of differently sized individuals have been discussed in several papers (cf. Werner, 1988; 1994; Lundberg and Persson, 1993). Empirical evidence that size-dependent competitive abilities may generate population cycles has also been provided (Hamrin and Persson, 1986; McCauley and Murdoch, 1987). In addition, a number of theoretical papers have considered the implications of stage-based competitive relationships for population dynamics (Ebenman, 1988; Cushing and Li, 1991, 1992; Nisbet and Onyiah, 1994). However, an explicit and complete treatment of how the ontogenetic scaling of foraging rate affects population dynamics is lacking.

In this paper, we analyse the effects of different ontogenetic scalings of foraging rate as the most variable component of competitive ability on the population dynamics in a size-structured one consumer—one resource model. We use a physiologically structured model, an approach that explicitly links the dynamics that takes place at the level of population to the behavior of individual organisms (Metz and Diekmann, 1986; Metz *et al*., 1988; DeAngelis and Rose, 1992; de Roos 1997). This modelling approach allows us to mechanistically link individual (size) dependent foraging rate and metabolic demands to population dynamics. We show further that the results of our modelling provide an understanding of the mechanisms behind the population oscillations in populations where intercohort interactions have been suggested to drive the dynamics of consumer-resource interactions. These examples include planktivorous fish, zooplankton and cikadas (Bulmer 1977; Hamrin and Persson 1986; McCauley and Murdoch 1987; Townsend *et al*., 1990).

2. THE PHYSIOLOGICALLY STRUCTURED MODEL

2.1. Consumer-Resource Dynamics

Our physiologically structured model is built along the lines advanced by Metz and Diekmann (1986; see also Metz *et al*., 1988; de Roos 1988, 1997; de Roos *et al*., 1990, 1992, 1997). These models are based on a state concept at each of two levels of organisation: an *i*-state which represents the state of the individual in terms of a collection of characteristic physiological traits (size, age, sex, energy reserves etc.), and a *p*-state which is the frequency distribution over the space of possible *i*-states (Metz and Diekmann, 1986; Metz *et al*., 1988; Caswell and John, 1992; DeAngelis and Gross, 1992).

We have formulated our model in "cumulative" terms (see Diekmann *et al*., 1993, 1995), as opposed to the traditional approach based on instantaneous rates.

In the model, the consumer population is size-structured whereas the resource population is not. We assume that the resource is continuously reproducing throughout the season. The consumer is assumed to grow (or shrink in case of starvation) continuously during the season, but reproduces at discrete time instants only. The growth season of the consumer corresponds to the summer in the temperate region and reproduction takes place at the start of the growing season (i.e. spring). In the present paper, we ignore the winter season which is equivalent to the situation when winter adds nothing but a scaling down of all rates. Our model is a combination of a continuous dynamical system, describing growth and survival of the consumer and production and consumption of the resource during summer, and a discrete map describing the pulsewise reproduction of consumers in spring. This combination takes the size distribution of the consumer population and the resource density at the beginning of a season to their corresponding values at the beginning of the next season. We thus have all the usual concepts of the theory of dynamical systems, e.g. "fixed point," "periodic orbit" and "attractor" to our disposal. For instance, a fixed point, or equilibrium, implies that the consumer size distribution and the resource density always has the same value at a fixed time within each season, even though during the season these will of course change. Similarly, an orbit of period p is a solution that repeats itself at a fixed time every pth season. In our analyses, we chose the end of the day prior to the reproductive event as reference time and consequently all results were extracted at this instant. At this particular time, it was possible to study reproductive investment of each consumer cohort in the population as well as the total number of offsprings produced the following day.

As is described above, the core part of the structured population model is a description of the individual behavior of the consumers, that is, individual feeding, growth, development, reproduction and mortality, as a function of the current state of both the environment (resource) and the individual itself. In the following sections we will discuss this model of individual energetics in more detail.

2.2. Individual State and Individual State Space

We assume that the consumer's foraging, metabolism, growth, survival, and reproduction for each given resource density can be described as functions of two physiological variables, irreversible and reversible mass. In irreversible mass x we include compounds like bones and organs which cannot be starved away by the consumer. In reversible mass y we include energy reserves such as fat, muscle tissue and gonads. These reserves may be used to cover basic metabolism during starvation. The total mass of the individual hence equals $x + y$. For a similar approach, see Broekhuizen *et al.* (1994).

We assume that there exists a fixed irreversible mass x_f (f for fertile) that distinguishes juveniles from adults. Individuals with $x \leqslant x_f$ are juveniles and individuals with $x > x_f$ are adults that can produce young. It is further assumed that there is a maximal ratio of reversible mass to irreversible mass and that this ratio is different for juveniles and adults as the latter also allocate mass to gonads. Denoting these ratios by q_j and q_a for juveniles and adults, respectively, the i-state space is contained in the set

$$\Omega = \{x_0 \leqslant x \leqslant \infty, 0 \leqslant y \leqslant y^*(x)\}, \tag{1}$$

where x_0 is the (given) minimum irreversible mass an individual can have (i.e. at birth) and

$$y^*(x) = \begin{cases} q_j x & \text{if} \quad x \leqslant x_f, \\ q_a x & \text{if} \quad x_f < x. \end{cases} \tag{2}$$

The law of mass allocation to be discussed in Section 2.4 imposes further restrictions on the collection of possible individual states which turns out to be substantially smaller than the set Ω. See Fig. 1.

2.3. Consumption Rate, Attack Rate, and Handling Time

We assume that a consumer captures the resource following a Holling type II functional response. In general, the attack rate and the handling time depend on both i-state variables in which case y functions as a measure of the condition of the individual. In this paper, however, we assume that the attack rate and the handling time only depend on x through the quantity

$$w = x + q_j x. \tag{3}$$

We do this as functional response experiments with size-structured consumers have shown a close relationship between capture rate and body length independent of body condition (Mittelbach 1981; Persson 1987). We call the quantity w effective body mass. The functional response is hence described by:

$$\gamma(w, R) = \frac{a(w)\, R}{1 + a(w)\, h(w)\, R}, \tag{4}$$

where $a(w)$ is the attack rate, $h(w)$ is the handling time, and R is the resource density.

For a given prey size, attack rate $a(w)$ has been found to be a hump-shaped function of predator size (Werner, 1988; Tripet, and Perrin 1994). The initial increase of the foraging capacity with predator size can be explained by an increase in visual acuity and locomotor ability, both of which will affect the encounter with prey (Schoener, 1969; Wilson, 1975; Peters, 1983; Noakes and Godin, 1988; Persson, 1987; Werner, 1988). The decreasing part of the function can be related to a decrease of rod density and hence the capacity to discern small prey (Breck and Gitter, 1983). Furthermore, attack efficiency may also decrease above a given body size due to decreased ability to make fine tuned manoeuvres (Hyatt, 1979; Breck and Gitter, 1983; Persson, 1987; Noakes and Godin, 1988). Adopting this general shape, we assume that the attack rate depends on effective body mass according to the following formula:

$$a(w) = A\left(\frac{w}{w_o}\exp\left(1-\frac{w}{w_o}\right)\right)^{\alpha}, \tag{5}$$

which relationship is governed by three (positive) parameters: (1) the maximum rate, A, (2) the body size at which the maximum rate is achieved, w_o, and (3) a size scaling exponent, α, which affects the rate by which the attack rate increases below and decreases above w_o. For large values of α the attack rate will increase more rapidly with w and have a sharp peak, whereas the attack rate will increase slowly with w and have a broad peak for small values of α (Fig. 2a).

Commonly, handling time $h(w)$ per prey first decreases with body size due to an increase in gape size and digestive capacity (Mittelbach, 1981; Hoyle and Keast, 1987; Persson, 1987) (Fig. 2b). Thereafter handling time increases; possibly due to difficulties in handling small prey (Persson, 1987). The specific function we use to describe this pattern is:

$$h(w) = \chi_1 + \chi_2 w^{-\chi_3}\exp(\chi_4 w), \tag{6}$$

where χ_1, χ_2, χ_3 and χ_4 are positive constants. The handling time has a minimum when $w = \chi_3/\chi_4$.

2.4. Mass Allocation, Growth, Reproduction, and Survival

Based on Peters (1983), Calder (1984) and Lundberg and Persson (1993), we assume that the metabolic demands per unit of time E_m as a function of body mass $x + y$ can be described by a power function:

$$E_m(x, y) = m_1(x + y)^{m_2}, \tag{7}$$

where m_1 and m_2 are positive constants. The net mass intake per unit of time $E_g(x, y, R)$ equals the mass intake per unit of time E minus metabolic demands per unit of time, hence

$$E_g(x, y, R) = E(w, R) - E_m(x, y), \tag{8}$$

where $E(w, R)$ equals the consumption rate $\gamma(w, R)$ multiplied by a conversion factor k_l which takes into account prey weight, assimilation efficiency and other conversion costs (Table I). If mass intake exceeds costs for metabolism, the surplus mass is invested in growth. We assume that a fraction, $\kappa(x, y)$, of the surplus mass E_g is allocated to growth in irreversible mass (and the rest into growth of reversible mass) according to the functions:

$$\kappa(x, y) = \begin{cases} \dfrac{1}{(1+q_j)\,q_j}\dfrac{y}{x} & \text{if} \quad x \leqslant x_f \\ \dfrac{1}{(1+q_a)\,q_a}\dfrac{y}{x} & \text{if} \quad x > x_f \end{cases} \tag{9}$$

Individuals are assumed to be born with *i*-state (x_0, y_0) where $y_0 = q_j x_0$, that is, they are born with the maximum ratio of reversible mass to their irreversible mass (Fig. 1). As long as the individual does not starve, that is as long as $E_g \geqslant 0$, a juvenile individual will always have this maximum ratio of reversible versus irreversible mass. When reaching the size-dependent maturity $x = x_f$, it is assumed that the allocation function changes and that the individual in addition to fat reserves also allocates mass to gonads. The maximum amount of reversible mass for an adult individual is therefore proportionally larger and equals $q_a x$ (Table I, Fig. 1). In effect, the allocation rule (9) ensures that the individuals will approach this boundary but seldom reach it. The individual allocates mass surplus to reversible mass at a rate which is proportional to $(y^* - y)/y^*$ (see Eq. 9 and Fig. 1).

If the net mass intake, E_g is negative, the individual starves and reversible mass (but not irreversible mass) decreases (Fig. 1). We assume that the individual can stand a certain amount of starvation, down to the point when $y = q_s x$ before its death rate increases due to starvation. The rate of starving to death, $\mu_s(x, y)$, when the

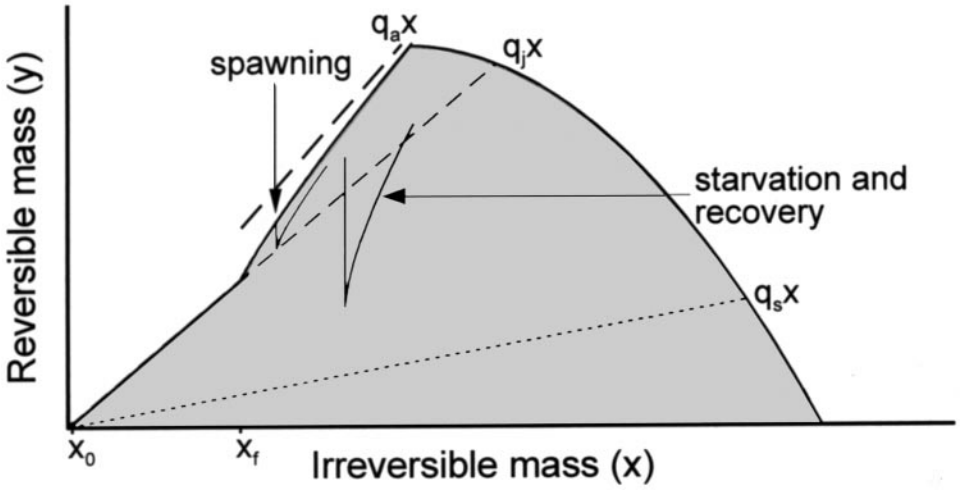

FIG. 1. The set of reachable individual states, as determined by the allocation of consumed energy to irreversible (x) and reversible (y) mass. The individual is born with an irreversible mass of x_0 and a reversible mass of $q_j x_0$ and will grow in mass along the line $y = q_j x$ as long as it does not starve. When reaching maturity (at irreversible size x_f), it increases its maximum amount of reversible mass to $q_a x$. When the individual spawns, reversible mass drops to $q_j x$ and after spawning the individual allocates mass according to the overall rule for partitioning between reversible and irreversible masses (Eq. 9). When starving, the individual only decreases in reversible mass, while during recovery after a starvation period, it allocates mass preferentially to reversible mass, as expressed by Eq. 9. Below the line $y = q_s x$, the individual starts to die of starvation. Observe that the individual may be positioned anywhere in the (x, y)-space (grey area) within the limits set by $y = q_j x$, $y = q_a x$, the x axis and to the right by the maintenance limit set by the solution for K from the equation $E_g(x, y, K) = 0$ (cf. Eq. 8).

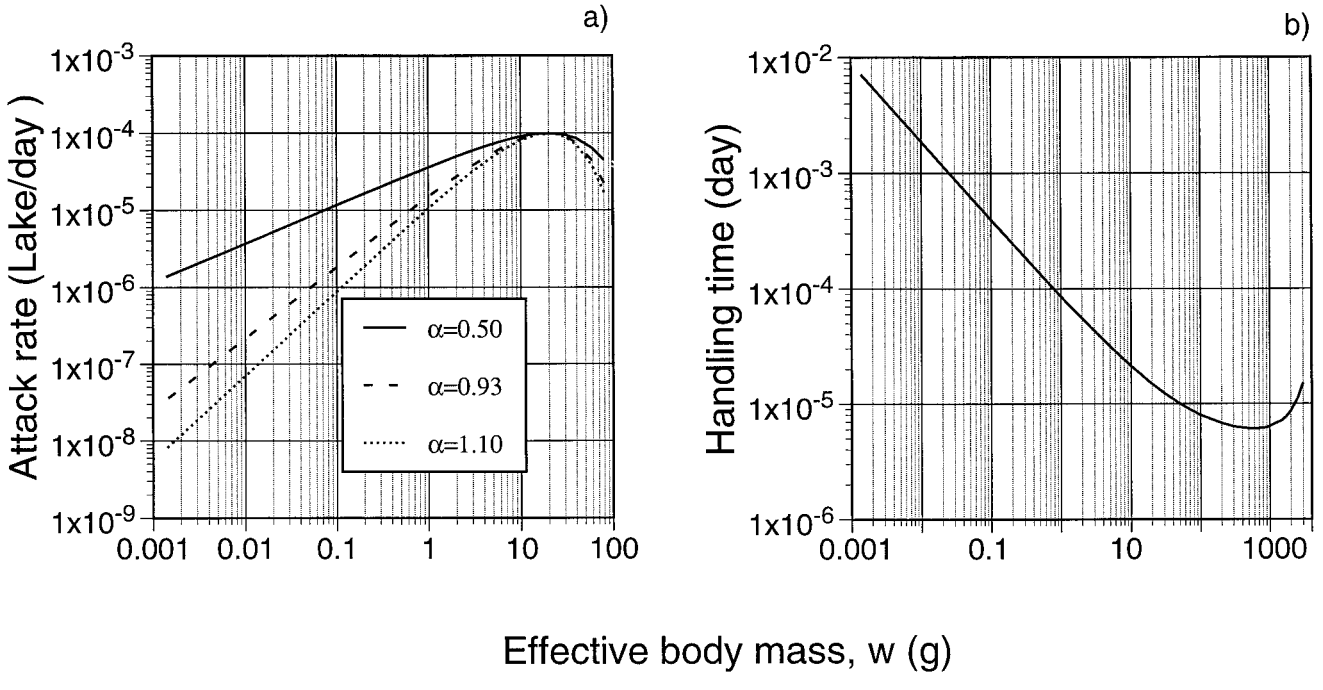

FIG. 2. Attack rate (a) and handling time (b) as functions of consumer effective body mass (w). For the attack rate function, curves for the three different α values used in the simulations are shown. Parameter values: $w_o = 17.42$ g wet weight and $A = 10^{-4}$ Lake day^{-1}. Other values as given in Table I.

reversible mass is below $q_s x$ is assumed to increase with the proportion x/y according to the following equation:

$$\mu_s(x, y) = \begin{cases} s\left(q_s \dfrac{x}{y} - 1\right) & \text{if } \dfrac{y}{x} \leqslant q_s \\ 0 & \text{if } \dfrac{y}{x} > q_s \end{cases} \qquad (10)$$

where s is a (positive) proportionality constant. This equation ensures that death is certain before $y = 0$.

In addition to starvation mortality, we assume that the individual may die of other causes than starvation at a rate μ_0 which is independent of the *i*-state. The total per capita death rate is thus the sum of the starvation and background death rates.

As described above, adult individuals allocate mass to gonads and hence have a relatively higher maximum reversible mass value than juveniles. The amount $y - q_j x$ of reversible mass exceeding $q_j x$ at the end of the growing season is used for reproduction. This gonad mass is transformed into newborns on the first day of the following growing season according to the birth function specified in the appendix and Table 1. At the same time, the parent's reversible mass is reduced to $y = q_j x$ (Fig. 1). If at the end of the growing season a mature individual's reversible mass is below $y = q_j x$, it will not reproduce.

2.5. The Model at the Population Level

At the population level the system under consideration constitutes a strongly coupled feedback loop between an unstructured resource and a size-structured consumer population. The resource population decreases in density due to the size-dependent foraging of the consumers and increases by means of an intrinsic growth process. We have assumed that this resource growth can be described by semi-chemostat dynamics. Semi-chemostat dynamics may be more realistic than the commonly used logistic growth dynamics when (1) the resource has a physical refuge or (2) the resource includes invulnerable (smaller), albeit mature size classes which grow into a vulnerable size range. The latter is, for example, the case for zooplankton fed upon by planktivorous fish. In turn, the resource density determines the current food intake by the consumers and hence indirectly governs consumer growth, reproduction and thus foraging capacity. It should be noted that semi-chemostat dynamics in the resource has a stabelising effect on the population dynamics compared to logistic growth dynamics (de Roos *et al.*, 1990).

Analytically, the model at the population level can be cast into the so-called cumulative formulation of physiologically structured population models (Diekmann *et al.*, 1993, 1995). This cumulative formulation uses measures (see appendix) to describe the state of the consumer population at a specific time, a variable R to refer to the resource density and integral equations to describe their dynamics. Essentially, the integral equations constitute a way of bookkeeping the dynamics of all individuals making up the population. In the appendix we give a full statement and discussion of the model equations. Here we restrict ourselves to sketching the representation of the model within the EBT (Escalator Boxcar Train) framework (de Roos, 1988 version 2.0; de Roos, 1993; 1997; de Roos *et al.*, 1992; see appendix for the formulation of the model in the EBT) that was used to carry out the numerical simulations. The EBT numerical method is specifically designed to handle the numerical integration of the equations that occur in physiologically structured models. The simulation results were verified by using different precisions in the numerical integrations re-running many of the parameter combinations used.

The pulsed reproduction process ensures that there exists a natural subdivision of the population into cohorts of individuals that all have the same age, reversible and irreversible mass. All individuals within a cohort are moreover assumed to grow at the same rate, i.e. individuals belonging to a given cohort do not diverge in their allocation to reversible and irreversible masses. The dynamics of every cohort can therefore be described by a system of ordinary differential equations, which keeps track of the number of individuals making up the cohort, their reversible mass and irreversible mass (see appendix). The dynamics of the entire consumer population, both in terms of its abundance and its state, can now be followed throughout the summer season by numerically integrating the system of ordinary differential equations for each cohort separately. In addition, changes in the resource population can be followed by numerical integration of the ordinary differential equation for the resource dynamics that incorporates the semi-chemostat growth and the total resource consumption. The latter equals the summed foraging rate over all cohorts. At the beginning of the season, new cohorts of individuals are added to the consumer population due to the reproductive process. This addition implies that the number of differential equations describing the population dynamics is increased. At the same time, the current value of the reversible mass in the cohorts of reproducing individuals is reset, reflecting their investment into offspring. Overall, the model simulations thus involve the numerical integration of a (large) system of ordinary

TABLE I

Definitions of Constants and Variables, and Their Numberical Values used in the Model

Symbol	Value	Unit	Description	References/comments
Enviroment				
T	90	day	Length of season, summer in temperature regions.	
Lake	10^9	L	Size of the lake.	
Resource				
R		ind 10^{-9} L^{-1}	Resource density.	
ρ	0.5*	day^{-1}	Resource growth, inflow rate. *ρ-value of 0.05 gave qualitatively similar results as 0.5.	
K	5 10^{10}	ind 10^{-9} L^{-1}	Carrying capacity.	
Consumer				
c		ind 10^{-9} L^{-1}g^{-2}	Consumer i-state distribution.	
A	varied	10^9 L day^{-1}	Maximum attack rate, i.e., at size w_o.	
α	varied		Size scaling exponent of the attack function.	
w_o	8.71, 17.42, 34.84	g	Effective body masses $w_o = x + q_j x$ at which maximum attack rate is atained.	
χ_1	4.0 10^{-6}	day	Constant used in the handling time function.	
χ_2	8.19 10^{-5}	day g^{x_3}	Constant used in the handling time function.	Lessmark (1983).
χ_3	0.68		Slope of decline in handling time at small consumer sizes.	
χ_4	1.15 10^{-3}	g^{-1}	Slope of increase handling time at large consumer sizes.	
m_1	0.033	g$^{(1-m_2)}$ day^{-1}	Metabolic constant.	
m_2	0.77		Metabolic exponent.	Schiemer *et al.* (1989), Kaufmann (1990), Keckeis and Schiemer (1990), Kock *et al.* (1992).
k_1	6.71 10^{-6}	g	Conversion factor; (assimilation efficiency ($=0.75$) − Specific Dynamic Action ($=0.14$))* prey mass ($=1.1\ 10^{-5}$ g).	
k_2	0.5		Conversion efficiency; converting reversible mass to offspring mass. Loss due to males not contributing to egg mass (30–35%), and costs for transforming somatic mass to gonad mass and gonad connective tissue (15–20%).	Assimilation efficiency Elliott (1976), SDA Beamish (1974).
ψ			New born size distribution, see also x_0. Three cohorts were used constituting 35%, 54%, and 11%, respectively.	
x_0	0.798, 0.804, 0.809	mg	Irreversible masses of the three size cohorts of newborn individuals. Total newborn mass becomes $w = x_0(1 + q_j)$.	Tong (1986), Wieser *et al.* (1998)
x_f	5.0	g	Maturation threshold in terms of irreversible mass.	
x		g	Irreversible mass.	
y		g	Reversible mass.	
q_j	0.742		Proportionality constant determining maximum juvenile reversible mass.	
q_a	1.0		Proportionality constant determining maximum adult reversible mass (including gonads). Yields a maximum gonadosomatic index (GSI) of 15% that compensates for the absence of males in the model.	GSI slightly lower that that found for female roach Goldspink (1979), Papageorgiou (1979).
q_s	0.2		Proportionality constant determining at which level of reversible mass starvation mortality starts.	
s	0.2	day^{-1}	Constant for starvation mortality. This value of s implies that, without food, the number of individuals in a starving newborn cohort does not approach zero before the reversible mass approaches zero.	
μ_0	0.01, varied	day^{-1}	Constant background mortality rate.	

differential equations, which is extended in dimension at the beginning of each season with a concurrent reset of some of the variables (see de Roos *et al.* 1992). The dimension of the system is reduced whenever the number of individuals in a given cohort has become negligible, at which time the differential equations for this particular cohort are removed.

3. MODEL PARAMETERIZATION

Our main interest was to investigate the effects of the size scaling of the attack function, $a(w)$, on the population dynamics of the consumer-resource system. Specifically we focused on, and hence varied, the parameters affecting the size scaling exponent α and the maximum attack rate A in the expression for $a(w)$ (Eq. 5). To a lesser extent, we also cover variation in the body size w_o at which maximum attack rate occurs (Table I). Furthermore, because background mortality turned out to have substantial effects on stability, we varied the mortality rate, μ_0, over a wide range of parameter values.

Although metabolic demands and handling time are parameterised for the interaction between a planktivorous fish population of roach *Rutilus rutilus* and a relatively small-bodied zooplankton population as resource (Table I), the model should generally be interpreted as describing the interaction between a small prey and its specialist size-structured predator. All parameter values are given in Table I. All rates representing dynamic processes were scaled to a daily basis. All parameter values related to energetics which were not varied are based on a reference temperature of 19°C. With this temperature, a year (season) in the model is assumed to last 90 days. As mentioned above, we ignore processes taking place during the winter season in the present paper. It should, however, be noted that a scaling down of all rate parameters to the same extent to account for the lower temperatures in winter is analogous to changing the length of the summer season. We have found no qualitatively new types of dynamics when varying the season length in our model.

In the model, all individuals are assumed to be a hybrid between males and females. We therefore adjusted the reproductive investment q_a to be intermediate between males and females (Table I). All consumer offspring are released and hatch simultaneously at the start of the biological season and the offspring start to feed immediately after birth. The size distribution Ψ of the newborn individuals is assumed to be rather clumped and for computational reasons we chose to represent Ψ by three discrete size cohorts.

4. DYNAMICS OF THE CONSUMER-RESOURCE MODEL

To delineate the parameter combinations of interest within the (α, A)-plane, we derived two necessary conditions for consumer persistence. First, under optimal feeding conditions (i.e. when the resource density equals K) newborn consumers should not starve to death, which requires $E_g(x_0, q_s x_0, K) > 0$. Second, maturing consumers (individuals whose irreversible mass x passes through the threshold x_f) must be able to build up at least a minimum of gonads, requiring $E_g(x_f, q_j x_f, K) > 0$. On a semi-logarithmic scale these boundaries consist of two straight lines with different slopes (see Fig. 3). The first condition yields the boundary to the right in Fig. 3 and the second the boundary at the bottom of Fig. 3. Numerical simulations verified that the actual persistence boundaries were close to the ones derived from the necessary conditions above. As w_o is increased, the intercept of the persistence boundary of newborns is shifted upwards whereas the slope of the persistence boundary of maturing individuals increases. The region of consumer persistence in the (α, A)-plane thus becomes smaller as w_o is increased.

Effects of α. The time series of consumer and resource density at the pre-reproductive census time in spring showed a wealth of dynamical patterns, ranging from stable fixed points, regular cycles, quasi-periodic dynamics on invariant closed curves to chaos. The transitions between stable fixed points and quasi-periodic dynamics indicated the occurrence of Hopf (Neimarck–Sacker) bifurcations, while transitions between regular cycles and chaotic dynamics exhibited a cascade of period-doubling bifurcations. To point out the effects of the ontogenetic scaling of foraging rate on populations dynamics and its consequences at the individual level, we will concentrate on the biological significance of three major types of dynamics that were most frequently found: recruit-driven cycles, equilibrium and non-recruit juvenile-driven cycles, exemplified by the population time series at three different α values (0.5, 0.93, 1.10). For the default background mortality ($\mu_0 = 0.01$) the recruit-driven and non-recruit juvenile-driven cycles had a cycle period of 7 years, although the characteristics of the dynamics do not depend on the cycle length (see the discussion on the effects μ_0 later in this section).

The type of dynamics found at a specific combination of α and A turns out to be strongly determined by the scaling of competitive ability with consumer size. As

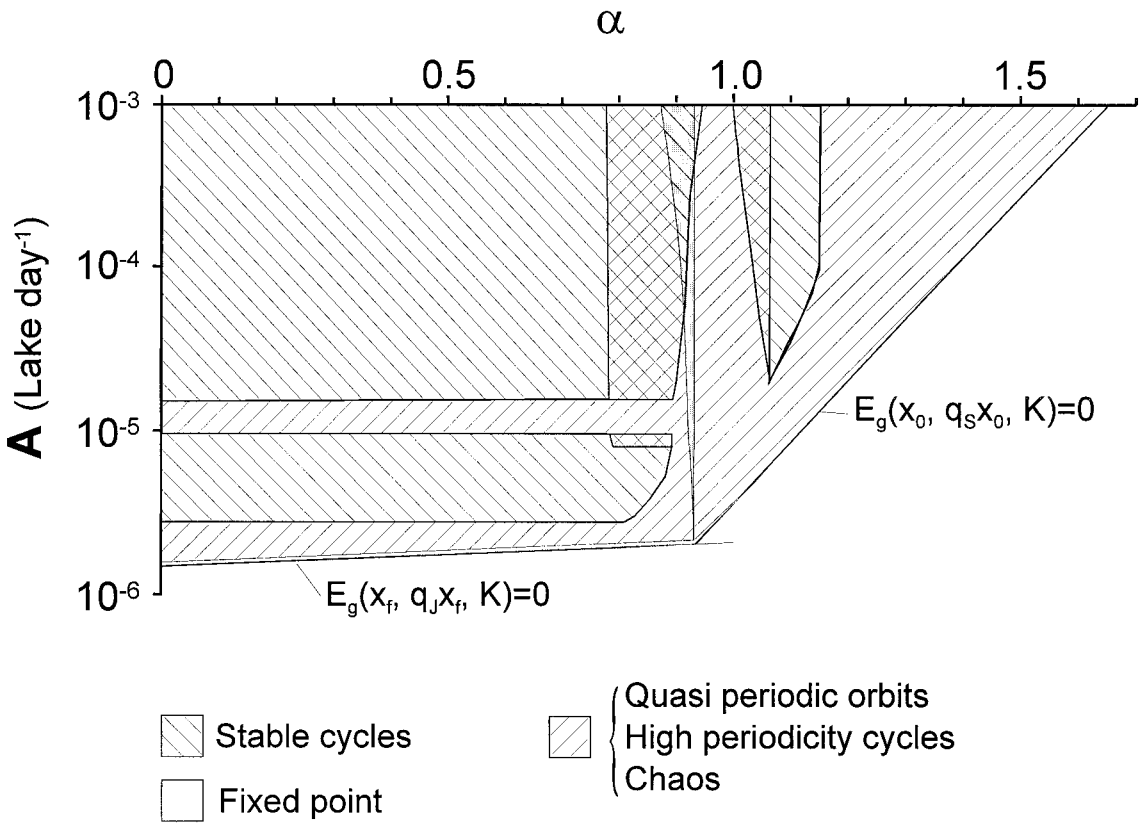

FIG. 3. Region in the (α, A)-plane bounded by the necessary conditions for consumer persistence. The lower and right-hand limits for persistence of the consumer constitute the solutions for α and A, for which $E_g = 0$ for a newborn individual of weight $x_0 + q_s x_0$, and for a maturing individual of weight $x_f + q_j x_f$, respectively, with the resource equal to its carrying capacity. Within the persistence region a broad classification of dynamics observed with semi-chemostat resource dynamics is given indicating the parameter combinations for which the 3 major types of dynamics (stable fixed point dynamics, recruit-driven and non-recruit juvenile-driven cycles) occurred and the parameter combinations for which other types of dynamics were found, such as quasi-periodic dynamics, cycles with higher periodicity (due to a period-doubling bifurcation) and chaotic dynamics. Both the recruit-driven and the non-recruit juvenile-driven cycles are indicated as stable cycles. All stable cycles for α values below 0.93 are recruit-driven cycles, while the stable cycles for higher a values are non-recruit juvenile-driven. Parameter values: $w_o = 17.42$ g wet weight, $K = 5\ 10^{10}$ Lake^{-1} and $\mu_0 = 0.01$ day^{-1}.

outlined in the introduction, competitive ability is a function of the ability of an individual to consume the resource and its ability to withstand resource depression (depending on metabolic demands). Specifically, the competitive ability of an individual of a given size can be characterised by the resource density at which it can just meet maintenance demands, that is, the solution for R from the equations $E_g(x, q_j x, R) = 0$. We will refer to this specific resource density as the *maintenance resource density*. We did not study variation in the functions for metabolic demands and handling, hence only changes in the parameters of the attack rate function (Eq. 5) will lead to changes in the competitive abilities of differently sized individuals. For relatively low α values ($\alpha < 0.9$) the maintenance resource density is monotonically increasing with body mass, for intermediate α values (i.e. α close to the intersection point, see Fig. 3) newborns and maturing individuals have similar maintenance resource densities and for high α values ($\alpha > 1$) the maintenance resource density first decreases rapidly with body mass and thereafter increases (Fig. 4). The α value at the intersection point of the existence boundaries of newborns and maturing individuals is the value of α at which the newborns and adults have similar competitive abilities (cf. Fig. 3). Hence, they cannot outcompete each other. At lower α values, the young-of-the-year have a higher competitive ability than the adults, and vice versa at higher α values.

Regular, Recruit-Driven Cycles. The regular cycles found at low α values ($\alpha = 0.5$) commenced with a strong reproduction of a newly matured age class (Fig. 5). The numerical dominance of recruits over adults caused a strong reduction of the resource level immediately after

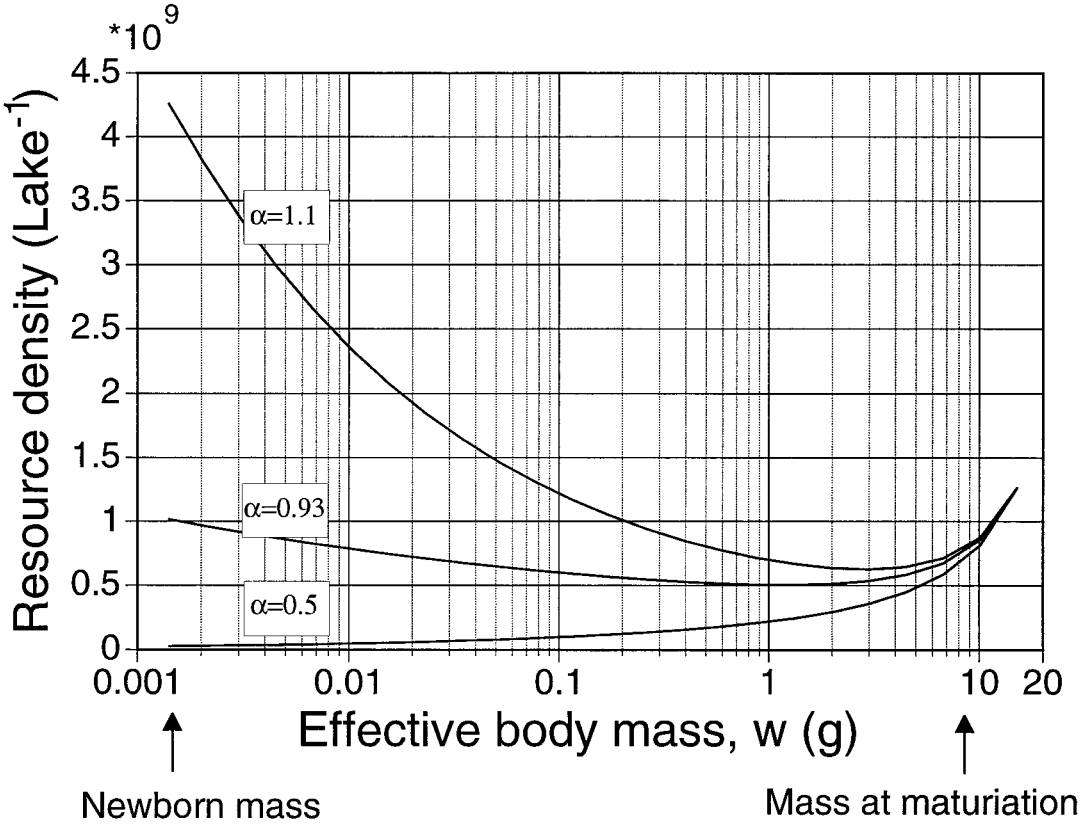

FIG. 4. Maintenance resource density (the solution for R from the equations $Eg(x, q_j x, R) = 0$) as a function of effective body mass for three different α values (0.50, 0.93, 1.10). Parameter values: $w_0 = 17.42$ g wet weight and $A = 10^{-4}$ Lake day^{-1}.

recruitment resulting in the adults starving to death (Fig. 5, 6). It was the combination of the newborn's relatively high attack rate (due to a low α, see Fig. 2a) and the swamping effect of offspring due to the pulsed reproduction in combination with high fecundity that made the resource level decrease below the level the adults need to grow (Fig. 4, 5). The newborns were able to grow at this low resource level due to their low maintenance resource density (Fig. 4, 5). The resource density remained below the adults maintenance resource density sufficiently long to cause the adults to starve to death. As a result, only cohorts belonging to one age class were present in the consumer population (Fig. 6). The growth of the individuals in this age class increased as the resource recovered from the initial decline. The individual growth rate and rate by which the resource population recovered was related to the disappearance of consumers due to background mortality. Hence, the cycles tend to become shorter with increasing background mortality (see below). When the juvenile cohort matured and reproduced, their offspring caused a dramatic decrease in the resource again leading starvation death of adults. As a result, the maximum size reached by adults was below w_o (17.42 g) and recruitment only occurred every 7th year (Fig. 5, 6). That is, the consumers were functionally semelparous despite being defined as iteroparous.

With increasing α, the competitive ability of the adults relative to the recruits increased as the recruits' ability to reduce the resource density declined. As a consequence, the adults managed to survive in the population for several years, although reproduction still only occurred every 7 years. Finally, at still higher α values, the adults succeeded in reproducing twice and the stable cycles collapsed into low-amplitude, quasi-periodic dynamics or a stable equilibrium depending on A and w_o (Fig. 3).

Stable Equilibria. At intermediate α-values ($\alpha = 0.93$) close to the α where the persistence boundaries intersected stable equilibria were observed (Fig. 5, 6). Annual recruitment was considerably lower than recruitment occurring in the recruitment year in the cycles (Fig. 7). The equilibrium resource density was just above the maintenance resource density for the newborns allowing coexistence between juvenile and adult cohorts (age

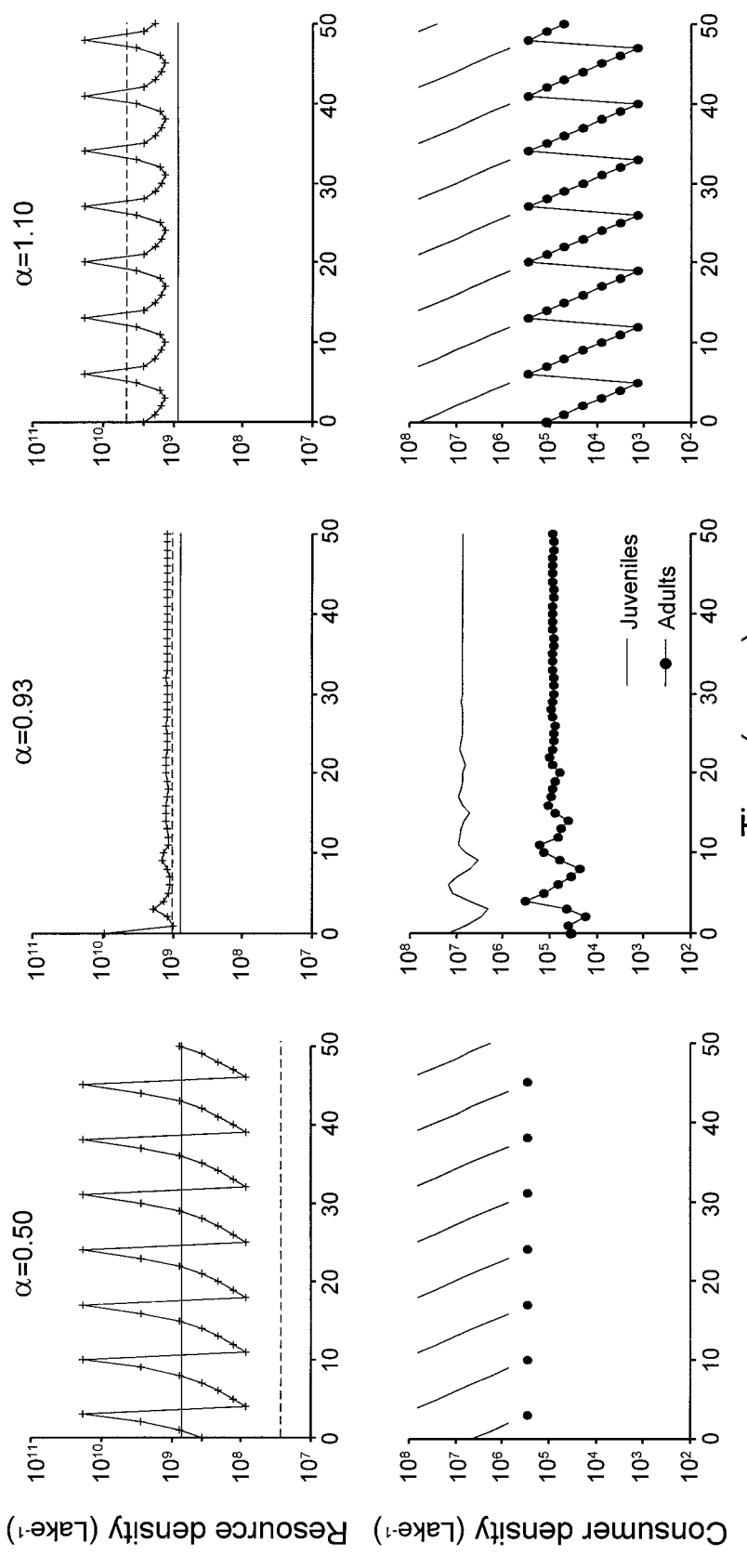

FIG. 5. Population dynamics in resource (above) and consumer (below) populations at three different α values (0.50, 0.93, 1.10) with semi-chemostat resource dynamics. The data represent the densities at the pre-reproductive census time in spring. For the consumer population, the size distributions have been collapsed into two cohorts, juveniles and adults. The inserted lines in the figures show the maintenance resource density ($E_g = 0$) of a recruit (mass $x_0 + q_j x_0$) (dashed line) and of a maturing individual (mass $x_f + q_j x_f$) (solid line). Parameter values: $w_o = 17.42$ g wet weight, $A = 10^{-4}$ Lake day^{-1}, $K = 5\,10^{10}$ Lake^{-1} and $\mu_0 = 0.01$ day^{-1}.

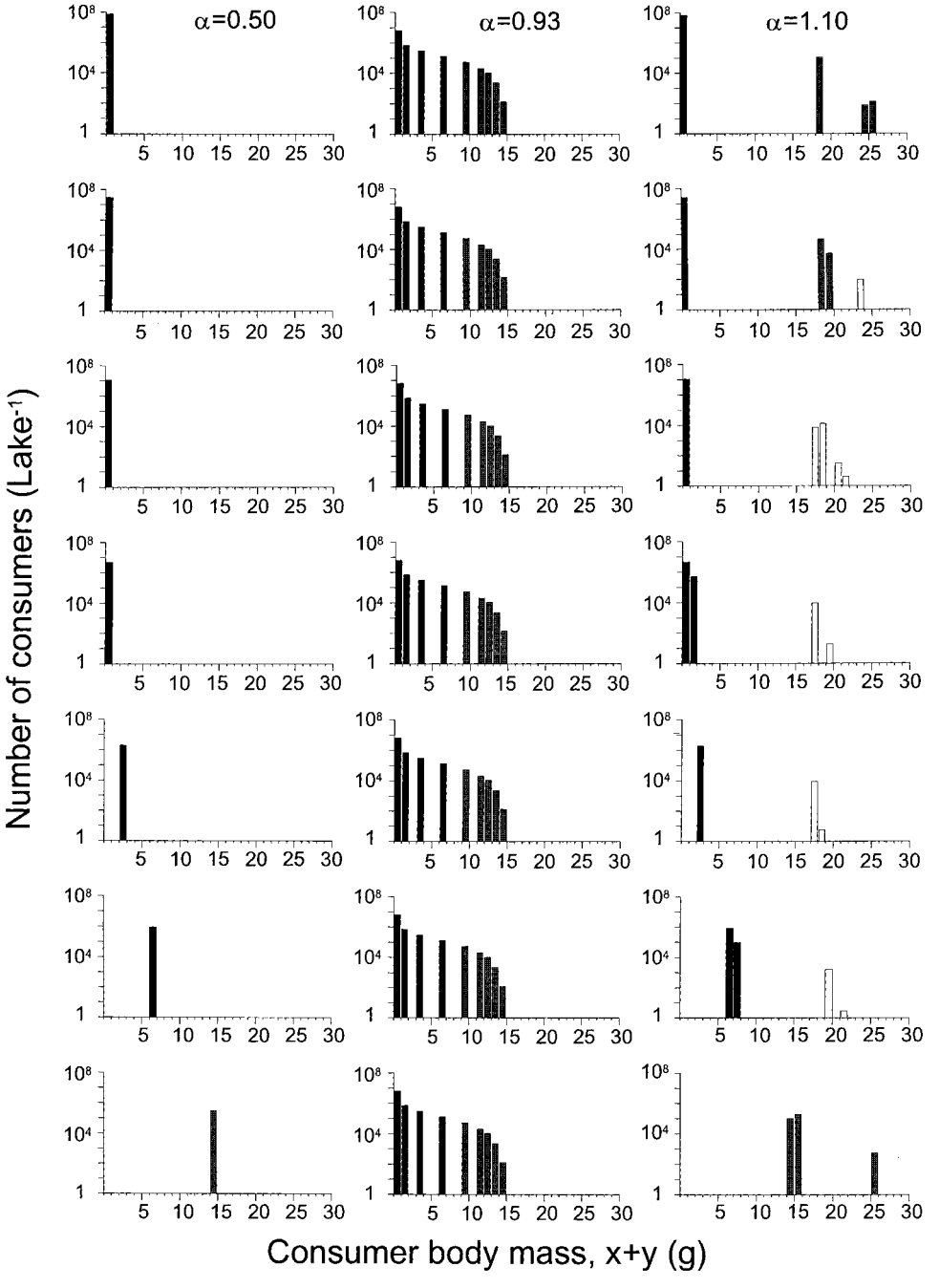

FIG. 6. Weight distributions of the consumer population in each year for the population dynamics shown in Fig. 5. The upper row represents the year in the cycle (if present) when recruitment occurs. Black histobars represent juveniles, grey histobars reproducing individuals and open histobars mature, but non-reproducing individuals. Note that individuals may shrink between years for $\alpha = 1.10$. Cohorts with less than one individual have been excluded.

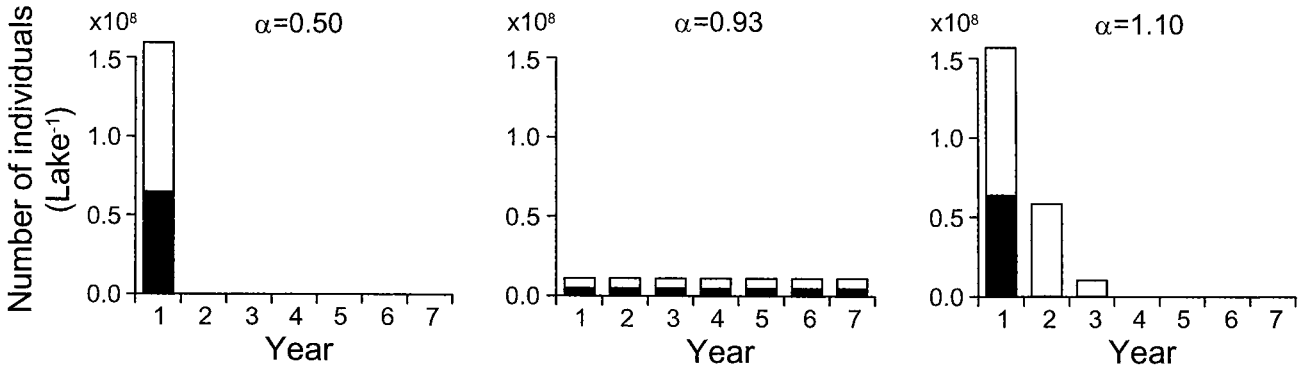

FIG. 7. The number of individuals recruited (whole histobars) and still alive 90 days after recruitment (black part of histobars) for the population dynamics shown in Fig. 5 and 6. The values at the x-axis represent the different years in the 7 year cycles present for $\alpha = 0.50$ and $\alpha = 1.10$, where year 1 refers to a year in which recruitment is successful.

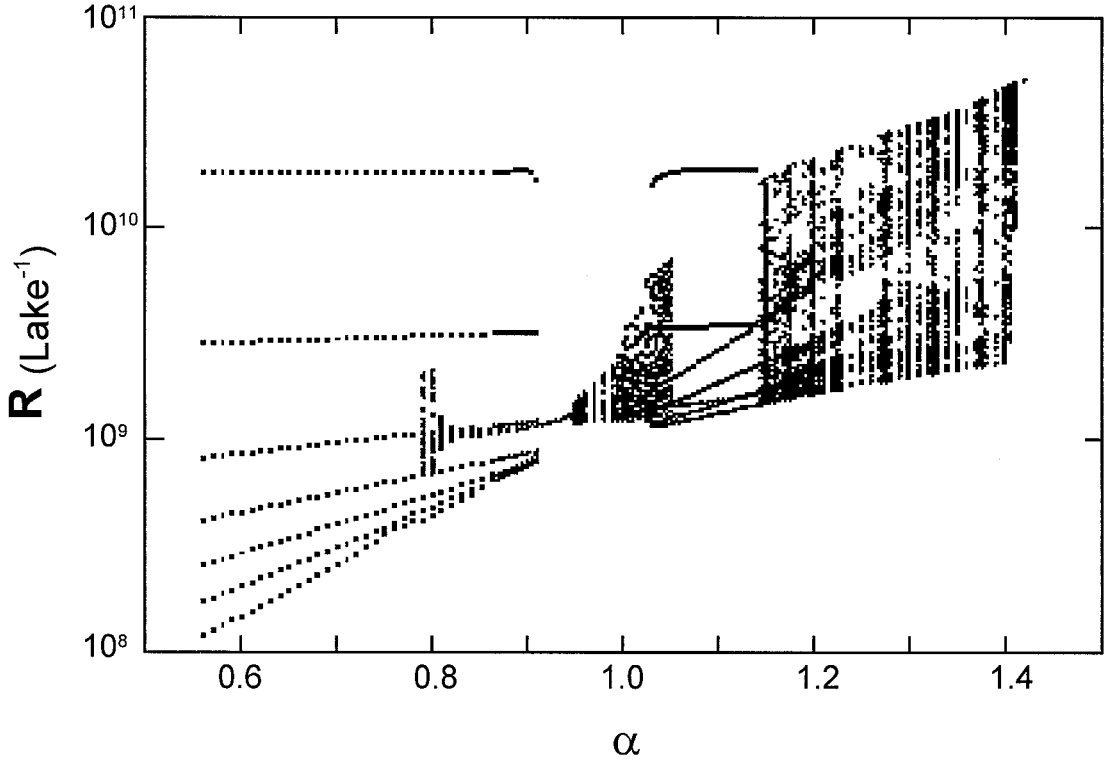

FIG. 8. Bifurcation plot of the resource density (R) versus the slope of the attack rate (α). The graph is compiled from the resource densities at the pre-reproductive census time in spring that were observed in the numerical simulations after transient dynamics had disappeared. The resource densities from these time series are represented with a dot plotted at the particular α-value. Other parameter values $w_o = 17.42$ g wet weight, $A = 10^{-4}$ Lake day^{-1}, $K = 5\ 10^{10}$ Lake^{-1}, and $\mu_0 = 0.01$ day^{-1}.

classes) (Fig. 4, 5, 6). An important factor contributing to the observed equilibrium conditions was that the maintenance resource density was relatively independent of body size over a wide range of body sizes preventing any size cohort from outcompeting the others (Fig. 4). Despite a resource density close to the maintenance limit, the consumers reached maturity after 6 years. The adults initially increased their reproductive output with size. After a few reproduction occasions, the gonads declined in size and the adults reached a stage where no further reproductive investment was possible. The maximum adult size was also in this region below w_o(17.42 g), but adult reproduction ceased because of the retardation in the increase in attack rate when body size approaches w_o (Fig. 2a). No starvation mortality was present for any cohorts within the stable equilibrium region, hence the background mortality totally determined the life span of the consumers.

Regular, Non-recruit Juvenile-Driven Cycles. The cycles at higher α values ($\alpha = 1.1$) to the right of the parameter region where stable equilibria occurred were similar to the cycles to the left of that region in that a strong juvenile year class matured and gave rise to a new strong recruit year class of similar size (Fig. 6, 7). However, due to the low attack rate of recruits (Fig. 2a), this strong year class could not depress the resource level to the same extent as could a strong recruit year class in the recruit-driven region where the attack rate of recruits was higher (Fig. 5). As a result, the adults could obtain enough energy to reproduce in the following next two years (Fig. 7). As the maintenance resource density of newborn individuals is high, offspring born in the years following a strong recruitment starved to death (Fig. 4, 7). The reason for the reappearance of the cycle is thus that at a certain α, previously recruited juveniles depress the resource to a level at which the newborns cannot survive despite the fact that that resource levels may allow the adults to produce gonads. The total feeding rate of the successfully entered strong year class increases during its first four years of life, because the individuals grow at

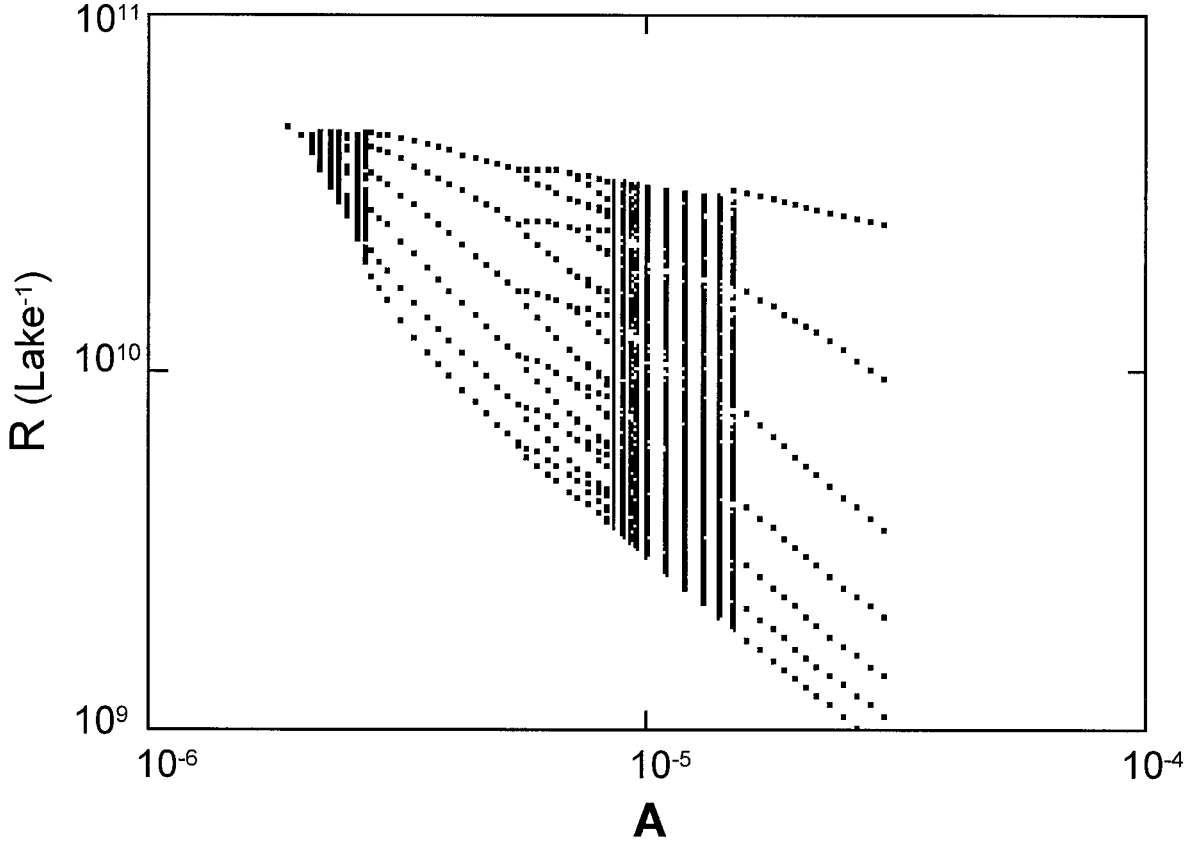

FIG. 9. Bifurcation plot of the resource density (R) versus the maximum attack rate (A). The graph is compiled from the resource densities at the pre-reproductive census time in spring that were observed in the numerical simulations after transient dynamics had disappeared. The resource densities from these time series are represented with a dot plotted at the particular A-value. Other parameter values: $w_o = 17.42$ g wet weight, $\alpha = 0.7$, $K = 5\ 10^{10}$ Lake^{-1}, and $\mu_0 = 0.01$ day^{-1}.

a rate fast enough to more than compensate for the decrease in their numbers due to background mortality. As a result, population consumption rate increased and the resource level continued to decrease for four years before it started to recover (Fig. 5). This situation contrasts to the one with recruit-driven cycles (Fig. 4, 5, 6). While the population dynamics at low α values was driven by recruits, the cycles at higher α values were thus driven by juveniles already recruited preventing new recruits to enter the system. This difference in dynamics between low and high α values can be related to the different forms of the relationship describing competitive ability as a function of body size (Fig. 4).

The adults reached larger sizes than under stable equilibrium conditions and the size often exceeded w_o. Consequently, the largest adults suffered from starvation during the years after a successful recruitment event which is revealed by the change in mass distribution for the largest cohorts during years 1–5 (Fig. 6). At still higher α values the stable cycles collapsed into chaotic dynamics, due to the reduced attack rate and hence capacity of a previously recruited juvenile year class to depress the resource density allowing the following year's offspring to be successfully recruited into the population (Fig. 3).

Figure 8 summarises these changes in the observed population dynamics with increasing α values. This bifurcation plot shows at every α value considered the resource densities at the pre-reproductive census time in spring that were observed in the numerical simulations after transient dynamics had disappeared. Stable, recruit-driven cycles with a period of 7 years persisted from low α-values (0.1) to α values slightly above 0.9 where the cycles collapsed into stable fixed point dynamics (Fig. 8). An alternative pattern of quasi-periodic dynamics was present from $\alpha \approx 0.8$, and bifurcated from the stable fixed point through a Hopf bifurcation at $\alpha \approx 0.9$. Increasing α above the stable parameter region more or less mirrored the previously described pattern, but the quasi-periodic fluctuations increased faster in amplitude than for the lower α values. The stable 7-year cycles with recruitment once every 7 year reappeared and gave rise to quasi-periodic dynamics for α values above 1.14. Finally, the consumer went extinct when reaching the boundary set by $E_g(x_0, q_s x_0, K) = 0$ (see Fig. 3).

Effects of A. Along a transect from low to high maximum attack rate (A) at $\alpha = 0.70$, the observed dynamics changed from a stable fixed point close to the lower persistence boundary set by $E_g(x_f, q_j x_f, K) = 0$ (see Fig. 3) to quasi-periodic dynamics, due to the occurrence of a Hopf bifurcation (Fig. 9). With increasing A, these quasi-periodic dynamics collapsed into stable 6 year cycles, which underwent a cascade of period-doubling bifurcations and finally gave rise to chaotic dynamics around $A = 10^{-5}$ Lake days. The consumer population consisted of several coexisting age classes for all these types of dynamics, although in the 6 years cycles the adult cohorts remaining in the population after a successful recruitment year were not capable of further reproduction due to their low reversible mass. When increasing A even further the chaotic dynamics collapsed into 7-year, recruit-driven cycles consisting of only one age class. The transition of stable, recruit driven cycles to chaotic dynamics around this value of A can be understood on the basis of the detailed description of the recruit-driven cycles discussed above. At this combination of α and A values, the newborn individuals are not capable of driving down the resource to a large extent. As a consequence, juveniles earlier enter the phase where they are more limited by their handling time than by their attack rate leading to an increased growth rate. The stable cycles collapse when the consumers are able to mature at an age of 6 years as the per capita fecundity of these 6-year old adults is low. As a consequence, resource depression by newborns is low as well and allows for another successful reproduction event of the adult cohort the following year.

We found that the same pattern of bifurcations occurs when varying the carrying capacity K of the resource (not shown here). Indeed, the population level equations presented in the appendix can all be rescaled by dividing

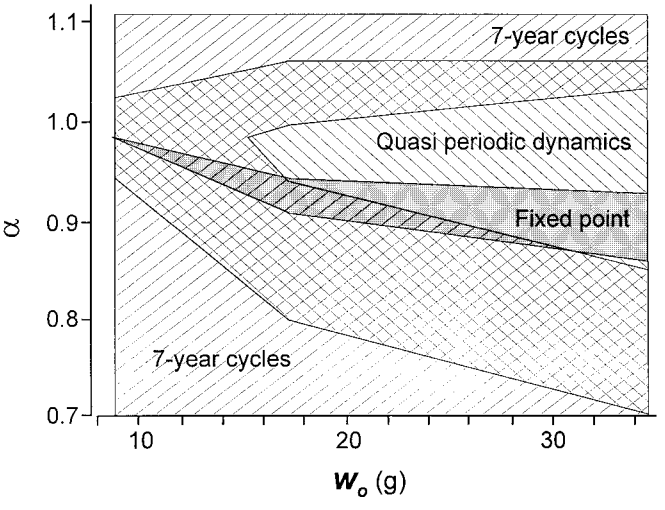

FIG. 10. Regions in the (α, w_o)-plane where different types of dynamics (7-year cycles, quasi-periodic dynamics, stable fixed points) occurred. The boundaries are drawn on the basis of simulations with $0.7 \leqslant \alpha \leqslant 1.1$, $w_o = 8.71$ (equal to the maturation size), 17.42 and 34.84 g, $A = 10^{-4}$ Lake day^{-1}, $K = 5\ 10^{10}$ Lake^{-1} and $\mu_0 = 0.01$ day^{-1}.

both the resource and the consumer densities by K. The parameters A and K in these scaled population equations occur always together as the product AK, implying that equivalent changes in either A or K should induce the same changes in the observed population dynamics.

Figure 3 summarises the regions in the (α, A)-plane where the different types of population dynamics occurred. Stable fixed point dynamics appeared along the lower boundary set by $E_g(x_f, q_f x_f, K) = 0$, which is a necessary condition for adult allocation to gonads, and along a minor part of the right boundary set by $E_g(x_0, q_s x_0, K) = 0$, which is a necessary condition for newborn growth. Stable fixed point dynamics was moreover found in a region expanding above the intersection point of these two boundaries. Most prominent is the extensive set of parameter combinations for which stable, recruit-driven cycles occur.

Effects of w_o. The ontogenetic scaling of the foraging rate we are concerned with in this paper also includes the effects of w_o, the size at which the maximum attack rate is achieved. Changes in w_o are negatively correlated with the extent of the region in the (α, A)-parameter space, for which consumers can persist. Also the regions with the different types of dynamics are affected by varying w_o. With decreasing w_o the region of consumer persistence expands mainly because the persistence boundary of newborns is shifted (the right-hand boundary in Fig. 3). w_o has, moreover, pronounced effects on the regions where stable equilibrium and quasi-periodic dynamics occur (Fig. 10). As w_o decreases towards the effective body size at maturation, $x_f + q_j x_f$ the parameter region where stable equilibria occur becomes narrower and moves towards larger α values. When w_o equals the effective body size at maturation, no stable equilibrium with consumer-resource coexistence are found. As w_o decreases, quasi-periodic dynamics occur over a narrower range of α values, and the α value at which the quasi-periodic orbits collapse into recruit-driven cycles increases (Fig. 10). In contrast, the α value at which the quasi-periodic dynamics collapse into non-recruit juvenile-driven cycles is less affected by a change in w_o. When w_o approaches the effective body size at maturation, the region with stable cycles persists in the entire range of α values analysed (Fig. 10). This pattern results from the fact that a decrease in w_o will decrease the scope for adults to reproduce several times. The postulated connection between several reproductive events (functional iteroparity) and the presence of stable fixed point

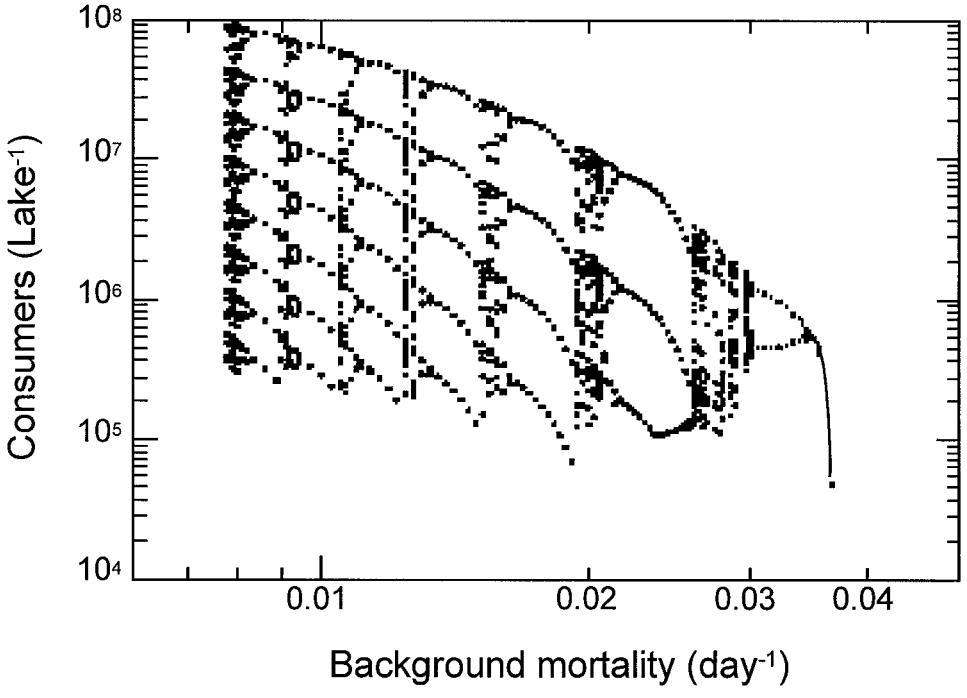

FIG. 11. Changes in the length of the recruit-driven cycles in relation to the background mortality rate μ_0. The graph is compiled from the consumer densities at the pre-reproductive census time in spring that were observed in the numerical simulations after transient dynamics had disappeared. The consumer densities from these time series are represented with a dot plotted at the particular μ_0-value. With decreasing mortality rate regular cycles go through a cascade of period doubling bifurcations to chaotic dynamics prior to a prolongation of the cycle period with an extra year. Parameter values: $\alpha = 0.67$, $A = 10^{-4}$ Lake day^{-1}, $K = 5\ 10^{10}$ Lake^{-1} and $w_o = 17.42$ g.

dynamics is confirmed by an analysis of the behaviour of a modified semelparous version of the model. In this latter model, the cycles never collapse into stable fixed point dynamics independent of w_o. In contrast, chaotic dynamics are still present at high α values suggesting that the latter dynamics depend on the offspring size distribution (several cohorts present simultaneously) and not iteroparity per se.

Effects of μ_0. The background mortality (μ_0) has a major impact on the stability of the system and the periodicity of the recruit or non-recruit juvenile-driven cycles. In general, increasing μ_0 increases stability. At a sufficiently high μ_0 (0.033 for $\alpha = 0.67$), only stable fixed point dynamics occur (Fig. 11). Reducing μ_0 from this point leads to 2-year cycles, which, in turn undergo a series of period doubling bifurcations resulting in chaotic dynamics. At still lower μ_0, the chaotic dynamics change into 3-year cycles. This pattern repeats itself with further reduction in μ_0. After each phase of regular cycles, a cascade of period doubling bifurcations and chaotic dynamics, the newly appearing cycle is one year longer than the previous one (Fig. 11). The dominating period in the chaotic dynamics is the same as for the regular cycle.

Juveniles and adults can coexist whenever the population exhibits stable fixed point dynamics, 2-year cycles or 3-year cycles with μ_0 larger than 0.022. With 2-year cycles, reproduction occurs every year. With 3-year cycles, reproduction is absent for one of the three years at high μ_0, whereas reproduction only occurs once during the 3-year cycle at low μ_0. As a consequence, non-recruit juvenile-driven cycles do not occur with a period of 2 and 3 years. For regular cycles longer than 3 years, one reproductive occasion during a cycle is the rule. All cycles with a period longer than 3 years have similar characteristics as the 7-year cycles discussed in detail above.

5. DISCUSSION

5.1. Ontogenetic Scaling and Population Dynamics

Changes in individual size and morphology occur in almost all animal taxa and have profound consequences for the foraging capacity and metabolic requirements of organisms in different stages of their life. The effects of such ontogenetic scalings of foraging rate and metabolism on the outcome of competitive interactions between different organisms have been studied at the individual level, in, for example, anurans (Werner, 1994). To our knowledge, our paper is the first to address the consequences of these size-specific, individual-level differences at the population level in the case of pulsed, as opposed to continuous reproduction.

Our analysis shows major effects of the ontogenetic scaling of attack rate on the population dynamics, often leading to cohort-driven population fluctuations. The investigated model is based on size-dependent energy gathering (gain) in terms of size-dependent attack rate and handling time and size-dependent spending (costs) in terms of a size-dependent metabolism. It is the size dependency of the attack rate and metabolic functions (see Section 4) that leads to differences in competitive abilities between different life stages of the consumers. The value of the exponent for the size scaling of metabolic demands is relatively conservative between taxa (Peters, 1983; Calder, 1984; Werner, 1988). Therefore, it is mainly differences in the size-related components of the attack rate investigated in this paper that will lead to a different ontogenetic scaling of the individual's competitive ability.

The differences in competitive ability between different size classes lead to dynamic patterns which, over a large region of the parameter space, are characterised by dominance and suppression by a single cohort. Stable equilibria are, apart from close to the persistence boundaries or when background mortality is high, only found when the competitive ability is similar throughout the entire life cycle of an individual, otherwise population cycles are likely to occur. These cycles are of two forms that are nonetheless based on the same principle: one lifestage of individuals completely outcompeting the others. Recruit-driven cycles occur when the minimum resource density to just meet maintenance increases monotonically with body mass. In contrast, non-recruit juvenile-driven dynamics occur when this critical resource density is lowest for an intermediate body mass (Fig. 4, 5).

A number of empirical cases can be found in the literature that suggest the occurrence of recruit-driven dynamics. Regular or possibly damped population oscillations have, for example, been found in several fish species (Cryer *et al.*, 1986; Townsend 1989; Townsend *et al.*, 1990). These species include roach, for which we parameterized the functions for metabolic demands, handling time, fecundity and offspring size. Simulation of an age-based model and empirical studies of the population dynamics of roach suggest that the presence of cycles in this species depends heavily on a low adult survival rate due to high background and starvation mortality, because a high survival rate will allow individuals to

reach a size where they shift to other diets. This, in turn, will decrease the possibility for density dependent effects of recruits on adult fecundity to occur (Townsend *et al*., 1990). Our results suggest that the coupling between a high survival rate of adults and the absence of regular cycles may arise because adults then have more than a single successful reproduction event during their life. Accordingly, the absence of stable fixed point dynamics and the enlargening of the part of parameter space with cycles following a decrease in w_o are related to the fact that the scope for adult mass allocation to gonads is diminished.

A classical example of population oscillations in fish is found in zooplanktivorous cisco (vendace) (*Coregonus albula*) (Järvi,1930; Svärdson, 1956; Aass, 1972; Ustyogov, 1972; Viljanen, 1986; Hamrin and Persson, 1986; Salojärvi, 1987; Helminen *et al*., 1993; Auvinen, 1994). The cycle length in these populations are often 2 years but an oscillation period of 3 years or more are also present (Svardson 1956, Aass 1972). Empirical evidence that these cycles were recruit-driven comes from (i) the strong impact that a strong recruiting age class had on the zooplankton resource, (ii) the depression of the zooplankton resource which caused starvation in older cisco whereas recruits (young-of-the-year) cisco always had a positive growth, and (iii) the positive correlation between mortality rate and body size during periods with high resource limitation (Hamrin and Persson, 1986). There was also a positive correlation between the abundance of cisco, one year old and older, and zooplankton density which is not expected if the cycles were non-recruit juvenile-driven (cg. Fig. 5).

Single generation cycles caused by dominance of one cohort and suppression of adult fecundity as is the case in the recruit-driven cycles have also been found in *Daphnia*. Models of individual behaviour of *Daphnia* show that *Daphnia* foraging capacity scales to body mass with a slope which lies within the values (0.56–0.67) where recruit-driven dynamics is predicted by our model (Kooijman and Metz, 1984; McCauley *et al*., 1990; Gurney *et al*., 1990; de Roos *et al*., 1992; Kooijman, 1993). Additionally, analyses of laboratory cultures, stock tanks and lake populations of *Daphnia* corroborate the existence of single generation cycles driven by dominance and suppression of adult fecundity (Murdoch and McCauley, 1985; McCauley and Murdoch, 1987, 1990; McCauley *et al*., 1988; McCauley, 1993). McCauley and Murdoch (1987) also mention other systems which may exhibit single generation cycles driven by dominance and suppression.

The non-recruit juvenile-driven cycles as well as recruit-driven cycles in our analysis were specific in containing only one age class of juveniles. The available data cited above and a priori expectations advanced by Wilson (1975) suggest that the scaling exponent for search capacity to body mass in organisms is not likely to exceed 1 if only exploitative competition is considered (see also reviews of empirical data in Peters, 1983; Calder, 1984). Adding size-dependent interference competition is expected to increase the competitive ability (foraging rate) of larger individuals versus smaller ones, which is likely to increase the possibilities for non-recruit juvenile-driven cycles. Periodic cicadas in North America form one potential example of non-recruit juvenile-driven cycles. Although other mechanisms like predation (Hoppensteadt and Keller, 1976) have been advanced to explain the cycles in cicadas, Bulmer (1977) showed theoretically that despite the importance of predator satiation for synchronising the cicada cycles, predation can not cause them. Instead, he suggested that the cycles were driven by cohort competition where larger (older) individuals were competitively superior to the smaller ones as a size effect (interference) and because the larger individuals are most likely to be initially in position in the roots (pre-emptive competition). This argumentation is supported by the results of our consumer-resource model in that the only situation when recruits could be prevented to enter a system with regular cycles is the situation with non-recruit juvenile-driven cycles (Fig. 7, 11).

The ontogenetic scaling of foraging rate to body size varies considerably between taxa, but part of this variation has been suggested to consist of systematic differences between functional groups (Wilson, 1975; Sebens, 1982; Werner, 1988; Lundberg and Persson, 1993). As a growing body of literature is becoming available on the size scaling of foraging rate and metabolic demands within taxa (Werner and Gilliam, 1984; Sebens, 1982; Werner, 1988, 1994; Mittelbach, 1981; Kooijman and Metz 1984; Gurney *et al*., 1990, McCauley *et al*., 1990; Jones, Richards and Southern 1992: Kooijman, 1993), it will be possible to analyse whether such systematic differences in the ontogenetic scaling of foraging rate can actually be corroborated. This would, in turn, allow predictions to be advanced regarding functional group dependent population dynamics.

5.2. Population Oscillations versus Stability

According to our analysis, one would expect many species to exhibit large population fluctuations which is a situation not commonly seen in nature. In this section we will consider some factors which will lead to large population fluctuations and discuss some other factors

that have the potential to stabilise the dynamics. The occurrence of the cycles depends heavily on a sufficiently high reproduction pulse to allow either the recruiters to reduce the resource more than the older cohorts (recruiter driven- dynamics) can, or non-recruit juveniles to reduce the resource more than recruiters (non-recruit juvenile-driven dynamics) are capable of. The seasonal reproduction *per se* is not a necessary requirement for the cohort-driven cycles to be present (see de Roos *et al*., 1990 for a continuous case), but these are more easily introduced and far more prominent in systems with discrete reproduction than in systems with continuous reproduction. When regular single generation cycles occur, their periodicity, T_C, must fulfil $T_C = Ln(F)/(\mu_0 Y)$, where F is the number of female offspring per adult female, Y is the season length in days, and μ_0 is the background daily mortality rate. This equation follows from the fact that on average only one of a parent's offspring must survive to reproduction to give rise to stable cycles. The regular cycles occur when the adults can build up sufficient fecundity, otherwise irregular or fixed point dynamics prevail (Fig. 11). Thus, for regular cycles to occur, the energy allocation must provide necessary space for gonad mass in combination with small offspring as in our model.

The periodicity of the cycles depends mainly on background mortality (see Fig. 11) while fecundity has less impact. On the basis of our results some effects of size dependent mortality can be outlined. For example, high mortality during the first few weeks after birth is expected to exert a stabilising impact on the dynamics, since the few surviving offspring will have a low impact on the resource and allow other cohorts to coexist. Size dependent mortality is commonly observed in natural populations (Litvak and Leggett, 1992; Fuijman, 1994; Fagan and Odell, 1996) and may be one important mechanism explaining the rare occurrence of the oscillating dynamics that are expected with a constant, size independent mortality. In such situations, the dynamical consequences of differences in competitive ability will not occur due to the absence of the necessary numerical effects. This will also be the case when the adults have a low fecundity.

Another potentially stabilising mechanism may be the presence of ontogenetic niche shifts (e.g. the presence of a second resource in the same or in another habitat). Changes in habitat use are likely to also affect the scaling of foraging rate to body size. For example, a predator searching for prey in a three dimensional environment (e.g. a pelagic habitat) is expected to have a higher size scaling of the foraging capacity to body size than the same predator searching for prey in a two dimensional environment (e.g. a benthic habitat). Correspondingly, the allometric relationship between encounter rate and body weight for bluegill sunfish (*Lepomis macrochirus*) decreased from 0.67 for pelagic prey, to 0.23 for vegetation prey to 0.09 for sediment prey (Mittelbach, 1981). In the context of ontogenetic niche shifts, it has also been suggested that there exists a connection between the parameters of the attack rate function and the extent to which organisms undergo ontogenetic niche shifts due to ontogenetic trade-off costs (Werner and Gilliam, 1984; Werner, 1988; Persson and Greenberg, 1990). To investigate the population dynamical consequences of these aspects in a one consumer—two resources system is an interesting topic for future research.

Acknowledgments The research has been sponsored by grants from the Swedish Council for Forestry and Agricultural Research to Mats Gyllenberg, Kjell Leonardsson and Lennart Persson, The Bank of Sweden Tercentenary Foundation to Mats Gyllenberg and the Swedish Natural Science Research Council to Lennart Persson. Valuable comments on the manuscript were given by Bill Murdoch and an anonymous reviewer.

APPENDIX

Cumulative Formulation of the Population Model

Here we give a description of the equations, defining the dynamical system at the population level. The irreversible mass of an individual will be indicated by X_R. The function $X_R(t, t_0, (x, y))$ specifies the amount of irreversible mass at time t of an individual which at time t_0 had an amount of irreversible and reversible mass equal to x and y, respectively. Therefore, the increase of irreversible mass during the time period between t_0 and t of such an individual equals

$$X_R(t, t_0, (x, y)) - x$$

For consistency reasons it is clear that

$$X_R(t_0, t_0, (x, y)) = x.$$

Analogously, the reversible mass of an individual will be indicated by Y_R. The function $Y_R(t, t_0, (x, y))$ specifies the amount of reversible mass at time t of an individual which at time t_0 had an amount of irreversible and

reversible mass equal to x and y, respectively. Again, it is clear that for consistency reasons:

$$Y_R(t_0, t_0, (x, y)) = y$$

On the basis of the model components at the individual level discussed in the main text, the equations describing the changes in the individual state can now be derived as functions of irreversible mass X_R, reversible mass Y_R, the time t, and resource density R. The growth in consumer irreversible mass is described by the following ordinary differential equation and initial condition:

$$\frac{d}{dt} X_R = \begin{cases} \kappa(X_R, Y_R)\, E_g(X_R, Y_R, R(t)), \\ \qquad \text{if} \quad E_g(X_R, Y_R, R(t)) > 0 \\ 0, \qquad \text{if} \quad E_g(X_R, Y_R, R(t)) \leqslant 0, \end{cases}$$

$$X_R(t_0, t_0, (x, y)) = x,$$

where the κ-function represents the mass allocation rule (Eq. 9) and the E_g-function (see Eq. 8) represents the net resource uptake. The above equation reflects our assumption that a fraction κ of the net energy production is channelled to the increase in irreversible mass, unless net production is negative, in which case the amount of irreversible mass does not change. The corresponding equations for the growth in reversible mass are:

$$\frac{d}{dt} Y_R = \begin{cases} (1-\kappa(X_R, Y_R))\, E_g(X_R, Y_R, R(t)), \\ \qquad \text{if} \quad E_g(X_R, Y_R, R(t)) > 0 \\ E_g(X_R, Y_R, R(t)), \\ \qquad \text{if} \quad E_g(X_R, Y_R, R(t)) \leqslant 0, \end{cases}$$

$$Y_R(t_0, t_0, (x, y)) = y.$$

which reflect our assumption that the remaining part $(1-\kappa)$ of net energy production is channelled to an increase in reversible mass. All deficits in net energy production are deducted from the reversible mass.

The probability that an individual with an amount of irreversible and reversible mass equal to x and y, respectively, at time t_0 will survive at least until time t, will be indicated with the function $F_R(t, t_0, (x, y))$. This probability is given by the following equation as a function of time, the background mortality rate μ_0, and the state dependent starvation mortality function $\mu_s(x, y)$:

$$F_R(t, t_0, (x, y)) = \exp\left(-\mu_0(t-t_0) - \int_{t_0}^{t} \mu_s(X_R(\tau, t_0, (x, y)), Y_R(\tau, t_0, (x, y)))\, d\tau \right).$$

The first term in the exponent relates to the background mortality over the time interval from t_0 to t, while the second term is the integrated result of starvation mortality during this period.

The dynamics of the consumer population within a season is given by the equation:

$$c(t)(w) = \int_{\{(x, y) \in \Omega:\, (X_R(t, t_0, (x, y)),\, Y_R(t, t_0, (x, y))) \in w\}} F_R(t, t_0, (x, y))\, c(t_0)(dxdy).$$

Here, $c(t)(w)$ represents the number of consumers at time t with an individual state (e.g. a combination of reversible and irreversible mass) within the set w. Similarly, $c(t_0)(dxdy)$can be interpreted as the number of consumers that at time t_0 have a combination of irreversible and reversible mass within a small subset $dxdy$. The integral expression thus reflects the simple bookkeeping fact that all individuals ending up at time t with an individual state within w are those that started out at time t_0 with an individual state somewhere in the individual state space Ω, in addition survived during the time period from t_0 to t and grew to end up with an individual state in w.

The resource balance within a season is a function of the initial resource density $R(t_0)$, the resource inflow rate ρ, the carrying capacity K, the consumer feeding rate function $\gamma(x, y)$, its survival probability $F_R(t, t_0, (x, y))$, and the consumer density. Its dynamics is given by:

$$R(t) = R(t_0) + \rho K(t-t_0) - \rho \int_{t_0}^{t} R(\tau)\, d\tau - \int_{\Omega} \int_{t_0}^{t} \gamma(X_R(\tau, t_0, (x, y)), Y_R(\tau, t_0, (x, y)), R(\tau))\, F_R(\tau, t_0, (x, y))\, d\tau c(t_0)(dxdy).$$

This equation specifies that the change in resource density over the period from t_0 to t equals the inflow term of the assumed chemostat dynamics $\rho K(t-t_0)$, minus its outflow over this period, which equals $\rho \int_{t_0}^{t} R(\tau)\, d\tau$, minus the total amount of consumption by the consumer population over the period. This total amount of resource consumed is given by the last integral in the

equation above. The integrand in this term represents the product of the number of consumers at time t_0 with an individual state in a small subset $dx\,dy$, their survival probability $F_R(\tau, t_0, (x, y))$ up to time τ and their feeding rate $\gamma(x, y)$ at this last point in time. The integral hence accumulates the feeding contributions over the period from t_0 to t of all consumer individuals that at time t_0 had a combination of irreversible and reversible mass anywhere within the individual state space Ω.

The consumer population after each reproductive event, which is assumed to take place at the discrete times nT, is related to its state just before the event by the function $b(x, y)$. This function describes not only the production of offspring but also the instantaneous change in the reversible mass of the reproducing adults. Hence, the consumer population before and after the reproductive event fulfils the equation:

$$c(nT+) = \int_{\Omega} b(x, y)\, c(nT-)(dxdy), \qquad n = 1, 2, ...,$$

where $b(x, y)$ is given by:

$$b(x, y) = k_2(y - q_j x)^+ \Psi + \delta_{(x,\, y-(y-q_j x)^+)}.$$

The first term in this expression reflects the assumption that adults invest all reversible mass that they accumulated on top of the amount $q_j x$ into the production of offspring. The conversion efficiency of this investment equals k_2 and Ψ indicates the size distribution of the neonates. The second term in this equation contains the delta function $\delta_{(x, y)}$ which specifies that all adults which do invest in reproduction have an immediate decrease of reversible mass from their current amount y to the value $q_j x$.

Escalator Boxcar Train Formulation of the Population Model

To study the dynamics of the population model numerically, its equations were recast into the EBT (Escalator Boxcar Train) formulation (de Roos *et al.*, 1992). Because of the pulsed reproduction the consumer population is naturally divided into distinct cohorts of individuals. All individuals within a single cohort are born with the same irreversible and reversible mass. They also remain identical to each other throughout their lifetime because growth is deterministic. The consumer population hence consists of a finite number of cohorts of identical individuals.

A growing season is assumed to last T time units from $t = (n-1)\,T$ to $t = nT$ $(n = 1, 2, 3...)$. Within each growing season the resource density, the number of individuals in each consumer cohort, their irreversible and reversible mass all change continuously. Reproduction takes place at the beginning of the growing season at the discrete times $t = nT$. A discrete map describes the state of the consumer population after the reproduction event as a function of its prereproduction state. The EBT formulation of the population model is hence a combination of a continuous-time process, specified in terms of ordinary differential equations, and a discrete-time process, specified as a mapping (cf. model C, "the food-dependent, size-structured model," in de Roos *et al.*, 1992).

Let $N^i(t)$ denote the number of individuals in cohort i at time t, and $X^i_R(t)$ and $Y^i_R(t)$ the irreversible and reversible mass, respectively, of these individuals. Let there be M cohorts of individuals present. The within-season dynamics of all consumer cohorts and the resource density $R(t)$ is then governed by the following system of $(3M+1)$ ODEs:

$$\begin{cases} \dfrac{dN^i}{dt} = -(\mu_0 + \mu_s(X^i_R, Y^i_R))\, N^i \\ \dfrac{dX^i_R}{dt} = \begin{cases} \kappa(X^i_R, Y^i_R)\, E_g(X^i_R, Y^i_R, R) & \text{if } E_g(X^i_R, Y^i_R, R) > 0 \\ 0 & \text{if } E_g(X^i_R, Y^i_R, R) \leqslant 0 \end{cases} \quad i = 1 \cdots M \\ \dfrac{dY^i_R}{dt} = \begin{cases} (1-\kappa(X^i_R, Y^i_R))\, E_g(X^i_R, Y^i_R, R) & \text{if } E_g(X^i_R, Y^i_R, R) > 0 \\ E_g(X^i_R, Y^i_R, R) & \text{if } E_g(X^i_R, Y^i_R, R) \leqslant 0 \end{cases} \\ \dfrac{dR}{dt} = \rho(K-R) - \sum_{i=1}^{M} \gamma((1+q_j)\, X^i_R, R)\, N^i(t) \end{cases}$$

Starting at $t = 0$, which is assumed to be the beginning of a growing season, this system of ODEs is integrated numerically until $t = T$, corresponding to the end of the growing season. At $t = T$ reproduction takes place, described by the following mapping (T^- and T^+ in the next equations refer to the value of a variable directly before and after the reproduction event, respectively):

$$N^1(T^+) = 0.35B(T^-) \qquad N^2(T^+) = 0.54B(T^-) \qquad N^3(T^+) = 0.11B(T^-)$$
$$X_R^1(T^+) = 0.798 \qquad X_R^2(T^+) = 0.804 \qquad X_R^3(T^+) = 0.809$$
$$Y_R^1(T^+) = 0.592 \qquad Y_R^2(T^+) = 0.597 \qquad Y_R^3(T^+) = 0.6$$

$$\begin{cases} N^i(T^+ = N^{i-3}(T^-) \\ X_R^i(T^+) = X_R^{i-3}(T^-) \\ Y_R^i(T^+) = \begin{cases} q_j X_R^{i-3}(T^-) & \text{if} \quad X_R^{i-3}(T^-) > x_f \quad i = 3 \cdots M+3 \\ & \text{and} \quad Y_R^{i-3}(T^-) > q_j X_R^{i-3}(T^-) \\ Y_R^{i-3}(T^-) & \text{otherwise} \end{cases} \end{cases}$$

The first 3 cohorts represent newborn consumers, of which 35%, 54% and 11% have an initial irreversible mass $x_0 = 0.798$, 0.804, and 0.809, respectively. This distribution represents the newborn size distribution Ψ (see Table 1). The reversible mass of newborn individuals equals q_j times their irreversible mass. The function $B(T^-)$ represents the total population reproduction rate, given by:

$$B(T^-) = \frac{k_2}{(1+q_j)\,\bar{x}_0} \sum_{i=1}^{M} \begin{cases} Y_R^i(T^-) - q_j X_R^i(T^-) & \text{if} \quad X_R^i(T^-) > x_f \quad \text{and} \quad Y_R^i(T^-) > q_j X_R^i(T^-) \\ 0 & \text{otherwise} \end{cases}$$

Here $\bar{x}_0$ refers to the average irreversible mass of a newborn individual, calculated from the newborn size distribution Ψ (see Table I) as a weighted average over the three initial masses $x_0 = 0.798$, 0.804, and 0.809, respectively. The last equations of the reproduction mapping constitute a renumbering of all other cohorts and a reset of the reversible mass of adult, reproducing individuals to q_j times their irreversible mass, reflecting their contribution to the population birth rate $B(T^-)$.

The same mapping is applied at each of the reproduction events following $t = T^+$ (at $t = nT$, $n = 2$, 3...) while the dynamics from one reproduction event to the next (from $t = (n-1)\,T^+$ to $t = nT^-$) is always obtained by the numerical integration of the ODEs governing the within-season dynamics. In principle each reproduction event may thus lead to the addition of 3 new cohorts to the consumer population. The number of cohorts making up the consumer population is decreased if the number of individuals in a particular cohort has become negligibly small. Such cohorts are removed from the population.

REFERENCES

Aass, P. 1972. Age determination and years class fluctuations of ciscoe (*Coregonus albula*) in the Mjösa hydroelectric reservoire, *Rep. Inst. Freshw. Res. Drottningholm* **52**, 4–21.

Auvinen, H. 1994. "Intra- and Interspecific Factors in the Dynamics of Vendace (*Coregonus albula* (L.)) Populations," Ph.D. thesis, University of Helsinki, Finland.

Beamish, F. W. H. 1974. Apparent specific dynamic of largemouth bass, *Micropterus salmoides*, *J. Fish. Res. Board Can.* **31**, 1763–1769.

Beck, J. E., and Gitter, M. J. 1983. Effect of fish size on the reactive distance of bluegill (*Lepomis macrohirus*) sunfish, *Can. J. Fish. Aquat. Sci.* **40**, 162–167.

Broekhuizen, N., Gurney, W. S. C., Jones, A., and Bryant, A. D. 1994. Modelling compensatory growth, *Funct. Ecol.* **8**, 770–782.

Bulmer, M. G. 1977. Periodical insects, *Am. Nat.* **11**, 1099–1117.

Calder, W. A., III 1984. "Size, Function and Life History," Harvard Univ. Press, Cambridge.

Caswell, H., and John, A. M. 1992. From the individual to the population in demographic models, *in* "Individual-Based Models and Approaches in Ecology—populations, Communities and Ecosystems" (D. L. DeAngelis and L. J. Gross, Eds.), pp. 36–61, Chapman & Hall, New York.

Cryer, M., Peirson, G., and Townsend, C. R. 1986. Reciprocal interactions between roach, *Rutilus rutilus*, and zooplankton in a small lake: Prey dynamics and fish growth and recruitment, *Limnol. Oceanogr.* **31**, 1022–1038.

Cushing, J. M., and Li, J. 1991. Juvenile versus adult competition, *J. Math. Biol.* **29**, 457–473.

Cushing, J. M., and Li, J. 1992. Intra-specific competition and density dependent juvenile growth, *Bull. Math. Biol.* **54**, 503–519.

DeAngelis, D. L., and Gross, L. J., Eds. 1992. "Individual-Based Models and Approaches in Ecology—Populations, Communities and Ecosystems," Chapman & Hall, New York.

DeAngelis, D. L., and Rose, K. A. 1992. Which individual-based approach is most appropriate for a given problem, *in* "Individual-Based Models and Approaches in Ecology—populations, Communities and Ecosystems" (D. L. DeAngelis and L. J. Gross, Eds.), pp. 67–87, Chapman & Hall, New York.

De Roos, A. M. 1988. Numerical methods for structured population models: The escalator boxcar train, *Num. Meth. Part. Diff. Equations* **4**, 173–195.

De Roos, A. M. 1993. The escalator boxcar train—User's manual version 2.0, Department of Pure and Applied Ecology, University of Amsterdam, Amsterdam, Netherlands.

De Roos, A. M. 1997. A gentle introduction to physiologically structured population models, *in* "Structured Population Models in Marine, Terrestrial and Freshwater Systems" (S. Tuljapurkar

and H. Caswell, Eds.), pp. 119–204, Chapman & Hall, New York.

De Roos, A. M., Metz, J. A. J., Evers, E., and Leipoldt, A. 1990. A size dependent predator-prey interaction: Who pursues whom?, *J. Math. Biol.* **28**, 609–643.

De Roos, A. M., Metz, J. A. J., and Diekmann, O. 1992. Studying the dynamics of structured populations models: A versatile technique and its application to *Daphnia*, *Am. Nat.* **139**, 123–147.

Diekmann, O., Gyllenberg, M. M., and Thieme, R. H. 1993. Perturbing semigroups by solving Stieltjes renewal equation, *Diff. Integral Equations* **6**, 155–181.

Diekmann, O., Gyllenberg, M. M., and Thieme, R. H. 1993. Perturbing evolutionary systems by cumulative outputs an step responses, *Diff. Integral Equations* **8**, 1205–1244.

Ebenman, B. 1988. Dynamics of age- and size-structured populations: Intraspecific competition, *in* "Size-Structured Populations: Ecology and Evolution" (B. Ebenman and L. Persson, Eds.), pp. 127–139, Springer-Verlag, Heidelberg.

Ebenman, B., and Persson, L. 1988. Dynamics of age- and size-structured populations—an overview, *in* "Size-Structured Populations: Ecology and Evolution" (B. Ebenman and L. Persson, Eds.), pp. 3–9, Springer-Verlag, Heidelberg.

Elliott, J. M. 1976. The growth rate of brown trout (*Salmo trutta*) fed on reduced rations, *J. Anim. Ecol.* **44**, 823–842.

Fagan, W. F., and Odell, G. M. 1996. Size-dependent cannibalism in praying mantids: using biomass flux to model size-structured populations, *Am. Nat.* **147**, 230–268.

Fuijman, L. A. 1994. The interplay of ontogeny and scaling in the interactions of fish larvae and their predators, *J. Fish Biol.* **45**, 55–79.

Goldspink, C. R. 1979. The population density, growth rate and reproduction of roach (*Rutilus rutilus* L.) in Tjeukemeer, the Netherlands, *J. Fish Biol.* **15**, 473–498.

Gurney, W. S. C., McGauley, E., Nisbet, R. M., and Murdoch, W. W. 1990. The physiological ecology of *Daphnia*: A dynamic model of growth and reproduction, *Ecology* **71**, 716–732.

Hamrin, S. F., and Persson, L. 1986. Asymmetrical competition between age classes as a factor causing population oscillations in an obligate plaktivorous fish, *Oikos* **47**, 223–232.

Helminen, H., Auvinen, H., Hirvonen, A., Sarvala, J., and Toivonen, J. 1993. Year-class fluctuations of vendace (*Coregonus albula*) in Lake Pyhäjärvi, Southwest Finland, during 1971–1990, *Can. J. Fish. Aquat. Sci.* **50**, 925–931.

Hoyle, J. A., and Keast, A. 1987. The effect of prey morphology and size on handling time in a piscivore, the largemouth bass (*Micropterus salmoides*), *Can. J. Zool.* **65**, 1972–1977.

Hyatt, K. B. 1979. Feeding strategy, *in* "Fish Physiology" (W. S. Hoar, D. J. Randall, and J. R. Brett, Eds.), Vol. VIII, pp. 71–119, Academic Press, New York.

Hoppensteadt, F. C., and Keller, J. B. 1976. Synchronization of periodical cicada emergences, *Science* **194**, 335–337.

Jones, H. D., Richards, O. G., and Southern, T. A. 1992. Gill dimensions, water pumping rate and body size in the mussel *Mytilus edulis*, *J. Exp. Mar. Biol. Ecol.* **155**, 213–237.

Järvi, H. 1930. On the fluctuations in abundance exhibited by the stocks of lake herring (*Coregonus albula*) in Lake Keitle, Finland, *J. Cons. Explor. Perm. Internat. Mer.* **65**, 182–188.

Kaufmann, R. 1990. Respiration cost of swimming in larval and juvenile cyprinids, *J. Exp. Biol.* **150**, 343–366.

Keckeis, H., and Schiemer, F. 1990. Consumption, growth and respiration of bleak *Alburnus alburnus* (L.) and roach, *Rutilus rutilus* (L.), during early ontogeny, *J. Fish Biol.* **36**, 841–851.

Koch, F., Wieser, W., and Niederstätter, N. 1992. Interactive effects of season and temperature on enzyme activities, tissue and whole animal respiration in roach, *Rutilus rutilus*, *Envir. Biol. Fish* **33**, 73–85.

Kooijman, S. A. L. M. 1973. "Dynamic Energy Budgets in Biological Systems," Cambridge Univ. Press, Cambridge.

Kooijman, S. A. L. M., and Metz, J. A. J. 1984. On the dynamics of chemically stressed populations: The deduction of population consequences from effects on individuals, *Ecotox. Environ. Saf.* **8**, 254–274.

Lessmark, O. 1983. "Competition between Perch (*Perca fluviatilis*) and Roach (*Rutilus rutilus*) in South Swedish Lakes," Ph.D. thesis, Univ. of Lund, Sweden.

Litvak, M. K., and Leggett, W. C. 1992. Age and size-selective predation on larval fishes: The bigger-is-better hypothesis revisited, *Mar. Ecol. Progr. Ser.* **81**, 13–24.

Lundberg, S., and Persson, L. 1993. Optimal body size and resource density, *J. Theoret. Biol.* **164**, 163–180.

McCauley, E. 1993. Internal versus external causes of dynamics in a freshwater plant herbivore system, *Am. Nat.* **141**, 428–439.

McCauley, E., and Murdoch, W. W., 1987. Cyclic and stable populations: Plankton as a paradigm, *Am. Nat.* **129**, 97–121.

McCauley, E., Murdoch, W. W., and Watson, S. 1988. Simple models and variation in plankton densities among lakes, *Am. Nat.* **132**, 383–403.

McCauley, E., Murdoch, W. W., Nisbet, R. M., and Gurney, W. S. C. 1990. The physiological ecology of *Daphnia*: Development of a model of growth and reproduction, *Ecology* **71**, 703–715.

Metz, A. J., and Diekmann, O. 1986. "The dynamics of physiologically structured populations," Lecture Notes in Biomathematics, Vol. 38, Springer-Verlag, Heidelberg.

Metz, A. J., De Roos, A. M., and Van Den Bosch, F. 1988. Population models incorporating physiological structure: A quick survey of the basic concepts and an application to size-structured population dynamics in waterfleas, *in* "Size-Structured Populations: Ecology and Evolution" (B. Ebenman and L. Persson, Eds.), pp. 106–126, Springer-Verlag, Heidelberg.

Mittelbach, G. G. 1981. Foraging efficiency and body size: A study of optimal diet and habitat use by bluegills, *Ecology* **62**, 1370–1386.

Murdoch, W. W., and McCauley, E. 1985. Three distinct types of dynamics behaviour shown by a single planktonic system, *Nature* **316**, 628–630.

Murdoch, W. W., and McCauley, E. 1990. Predator-prey dynamics in environments rich and poor in nutrients, *Nature* **343**, 455–457.

Nisbet, R. M., and Onyiah, L. C. 1994. Population dynamics consequences of competition within and between age classes, *J. Math. Biol.* **32**, 329–344.

Noakes, D. L. G., and Godin, J. -G. J. 1988. Ontogeny of behavior and concurrent developmental changes in sensory systems in teleost fishes, *in* "Fish Physiology" (W. S. Hoar and D. J. Randall, Eds.), Vol. XIB, pp. 345–395, Academic Press, New York.

Nornberg, R. Å. 1988. Self-thinning of plant populations dictated by packing density and individual growth geometry and relationships between animal population density and body mass governed by metabolic rate, *in* "Size-Structured Populations: Ecology and Evolution" (B. Ebenman and L. Persson, Eds.), pp. 259–279, Springer-Verlag, Heidelberg.

Persson, L. 1985. Assymmetrical competition: Are larger animals competitively superior?, *Am. Nat.* **126**, 261–266.

Persson, L. 1987. The effects of resource availability and distribution on size class interactions in perch *Perca fluviatilis*, *Oikos* **48**, 148–160.

Persson, L. 1987. Assymmetries in competitive and predatory interactions in fish populations, *in* "Size-Structured Populations: Ecology and Evolution" (B. Ebenman and L. Persson, Eds.), pp. 203–218, Springer-Verlag, Heidelberg.

Persson, L., and Greenberg, L. A. 1990. Juvenile competitive bottlenecks: The perch (*Perca fluviatilis*)-roach (*Rutilus rutilus*) interaction, *Ecology* **71**, 44–56.

Peters, R. H. 1983. "The Ecological Implications of Body Size," Cambridge Univ. Press, Cambridge.

Polis, L. A. 1991. Complex trophic interactions in deserts: An empirical critique of food web theory, *Am. Nat.* **138**, 123–155.

Salojärvi, K. 1987. Why do vendace (*Coregonus albula* L.) populations fluctuate?, *Aqua Fenn.* **17**, 17–26.

Schiemer, F., Keckeis, H., and Wanzenböck, J. 1989. Foraging in cyprinids during early development, *Pol. Arch. Hydrobiol* **36**, 467–474.

Schoener, T. W. 1969. Models of optimal size for solitary predators, *Am. Nat.* **103**, 227–313.

Sebens, K. P. 1982. The limits to indeterminate growth: An optimal model applied to passive suspension feeders, *Ecology* **63**, 209–222.

Svärdson, G. 1956. Lambafjärdens siklöja, *Svensk Fiskeritidskrift* **65**, 73–80 [in Swedish].

Tong, H. Y. 1986. A qualitative and quantitative description of the early growth of roach *Rutilus rutilus*, in the laboratory, *Envir. Biol. Fish.* **15**, 293–300.

Townsend, C. R. 1989. Population cycles in freshwater fish, *J. Fish Biol.* **35**, 125–131.

Townsend, C. R., Sutherland, W. J., and Perrow, M. R. 1990. A modelling investigation of population cycles in the fish *Rutilus rutilus*, *J. Anim. Ecol.* **59**, 469–485.

Tripet, F., and Perrin, N. 1994. Size-dependent predation by *Dugesia lugubris* (Turbellaria) on *Physa acuta* (Gastropoda): Experiments and model, *Funct. Ecol.* **8**, 458–463.

Ustyogov, A. F. 1972. The ecological and morphological characteristics of the Siberian ciscoe (*Coregonus albula sardinella*) from the Yenisey basin, *J. Ichtyol.* **12**, 745–758.

Viljanen, M. 1986. Biology, propagation, exploitation and management of vendace (*Coregonus albula* L.) in Finland, *Arch. Hydrobiol. Beih. Ergebn. Limnol.* **22**, 73–97.

Werner, E. E. 1988. Size, scaling and the evolution of life, *in* "Size-Structured Populations: Ecology and Evolution" (B. Ebenman and L. Persson, Eds.), pp. 60–81, Springer-Verlag, Heidelberg.

Werner, E. E. 1994. Ontogenetic scaling of competitive relations: size-dependent effects and responses in two Anuran larvae, *Ecology* **75**, 197–231.

Werner, E. E., and Gilliam, J. F. 1984. The ontogenetic niche and species interactions in size-structured populations, *Ann. Rev. Ecol. Syst.* **15**, 393–425.

Werner, E. E., Mittelbach, G. G., Hall, D. J., and Gilliam, J. F. 1983. Experimental tests of optimal habitat use in fish: The role of relative habitat profitability, *Ecology* **64**, 1525–1539.

Wieser, W., Forstner, H., Schiemer, F., and Mark, W. 1988. Growth rates and growth efficiencies in larvae and juveniles of *Rutilus rutilus* and other cyprinid species: Effects of temperature and food in the laboratory and in the field, *Can. J. Fish. Aquat. Sci.* **45**, 943–950.

Wilbur, H. M. 1988. Interactions between growing predators and growing prey, *in* "Size-Structured Populations: Ecology and Evolution" (B. Ebenman and L. Persson, Eds.), pp. 157–172, Springer-Verlag, Heidelberg.

Wilson, D. S. 1975. The adequacy of body size as a niche difference, *Am. Nat.* **109**, 769–784.